

Lichen mimesis in mid-Mesozoic lacewings

Hui Fang^{1,2}, Conrad C. Labandeira^{1,2,3}, Yiming Ma¹, Bingyu Zheng¹, Dong Ren¹, Xinli Wei^{4*}, Jiayi Liu^{1*} and Yongjie Wang^{1*}

¹College of Life Sciences and Academy for Multidisciplinary Studies, Capital Normal University, Beijing 100048, China.

²Department of Paleobiology, National Museum of Natural History, Smithsonian Institution, Washington DC 20013, USA.

³Department of Entomology, University of Maryland, College Park, MD 20742, USA.

⁴State Key Laboratory of Mycology, Institute of Microbiology, Chinese Academy of Sciences, Beijing 100101, China

*For correspondence: wangyjosmy@foxmail.com (Y.W.), weixl@im.ac.cn (X.W.) and liu-jiax@263.net (J.L.).

Abstract

Animals mimicking other organisms or using camouflage to deceive predators are vital survival strategies. Modern and fossil insects can simulate diverse objects. Lichens are an ancient symbiosis between a fungus and an alga or a cyanobacterium that sometimes have a plant-like appearance and occasionally are mimicked by modern animals. Nevertheless, lichen models are almost absent in fossil record of mimicry. Here, we provide the earliest fossil evidence of a mimetic relationship between the moth lacewing mimic *Lichenipolystoechotes* gen. nov. and its co-occurring fossil lichen model *Daohugouthallus ciliiferus*. We corroborate the lichen affinity of *D. ciliiferus* and document this mimetic relationship by providing structural similarities and detailed measurements of the mimic's wing and correspondingly the model's thallus. Our discovery of lichen mimesis predates modern lichen-insect associations by 165 million years, indicating that during the mid-Mesozoic, the lichen-insect mimesis system was well established and provided lacewings with highly honed survival strategies.

Introduction

29 Modern insects have dramatic morphological specializations that match various objects of the
30 environment. For instance, the specializations occurring in katydids and butterflies that mimic leaves,
31 stick insects and inchworms that resemble twigs, and orchid mantids that duplicate orchid flowers,
32 provide ecological insights for understanding mimetic associations between insect mimics and their
33 plant models (*Stevens and Merilaita 2011; Gullan and Cranston 2014; Maran, 2017*). These and other
34 fascinating cases reveal that mimesis or camouflage is highly effective when cryptic insects resemble
35 closely the appropriate self-similar background, indicating the complexity of ecological relationships
36 between insect mimics and their imitating models. When and how insects first evolved such an
37 ingenious survival strategy is unclear. A Permian katydid exhibiting a mimicking pattern of wings
38 similar to the modern relatives was considered the oldest case of insect mimicry (*Garrouste et al.,*
39 *2016*). However, evidence for a contemporaneous mimetic relationship in this Permian deposit was
40 scarce, and there was no quantitative or other useful data to track the mimetic interactions among the
41 insect, model and predator. More recent cases of insect mimicry have been recorded from the Mesozoic,
42 indicating the existence of several such effective survival strategies. As in morphological
43 specializations involving masterly deceit found in modern insects, several Mesozoic insect taxa
44 developed remarkable structural adaptations resulting in highly accurate resemblances to co-existing
45 models (*Wang Y et al., 2012; Wang M et al., 2014; Yang et al., 2020*). Prominent among these mimetic
46 insects are Neuroptera (lacewings, antlions and relatives), a nonspeciose relic order consisting of ca.
47 6000 extant species that engaged in several, impressive instances of mimicry that reveal novel and
48 specialized strategies of deception, of which many are absent today. Striking examples are the Jurassic
49 lacewing *Bellinympha* (Saucrosmylidae), a compression fossil, mimicking cycadophyte leaves (*Wang Y*
50 *et al., 2010*), and larvae of the green lacewing *Phyllochrysa* (Chrysopidae) from amber, modified to

51 resemble co-occurring liverworts (*Liu et al., 2018*). Besides mimicry, other deceptive modes of
52 appearance have been documented among Mesozoic lacewings, such as camouflaged larvae of
53 chrysopid (green lacewing) and myrmeleontoid (antlion relative) neuropterans in amber, which evolved
54 distinctive debris-carrying behaviors to enhance their predatory effectiveness (*Pérez-de la Fuente et*
55 *al., 2012, 2018; Wang B et al., 2016; Badano et al., 2018*). These cases collectively have promoted
56 understanding of the early evolution of insect mimicry, but also have revealed that the currently species
57 poor Neuroptera had evolved a significant repertoire of specializations involving morphologies and
58 behaviors that adapted to a variety of Mesozoic settings.

59 In this report, we found an exceptional system of the first lichen mimesis by a fossil lacewing.
60 These occurrences are from the Daohugou 1 locality of Inner Mongolia in northeastern China. The new
61 lichen-like-mimicking insects represent a new genus with two new species and exhibit remarkable
62 wing patterns that accurately resemble the contemporaneous lichen species *Daohugouthallus ciliiferus*
63 Wang, Krings *et Taylor, 2010* (*Wang X et al., 2010*). The lichen affinity of the *D. ciliiferus* model
64 previously was doubted due to the absence of evidence for fungal and algal connections that would
65 indicate the presence of lichenization and thus the presence of a mutualistic symbiosis (*Honegger et al.,*
66 *2013; Lücking and Nelsen, 2018*). Our SEM results corroborate the actual presence of hyphae
67 connected to algal cells on the *D. ciliiferus* specimens, indicating the foliose and subfruticose lichen
68 growth forms were in existence during the Middle Jurassic. Present-day lichen-mimicking insects are
69 widely recorded among several diverse orders, especially Coleoptera (beetles), Lepidoptera (moths and
70 butterflies) and Orthoptera (grasshoppers, katydids and crickets), which have evolved unusual
71 specializations of morphology and behavior consistent with co-occurring lichens and other habitation-
72 or appearance similar organisms such as liverworts (*Gerson, 1973; Lücking, 2001; Capinera, 2008;*

73 *Cannon, 2010; Lücking et al., 2010*). An extraordinary orthopteran, the lichen dragon katydid from the
74 modern Ecuadorian Andes, provides an excellent disguise of lichens (*Braun, 2011*). Other predatory
75 and extant chrysopid larvae have a body mask adorned with affixed lichen fragments, an example of
76 aggressive mimicry or the “wolf in sheep’s clothing” syndrome (*Skorepa and Sharp, 1971; Slocum and*
77 *Lawrey, 1976; Wilson and Methven, 1997; Tauber et al., 2014*). Importantly, lichen-mimetic or
78 -camouflaged insects have established a specialized lichen-association for feeding or sheltering to
79 obtain survival advantage (*Gerson, 1973*). Our finding documents the earliest lichen-mimicking insect
80 and reveals that this strategy of mimicry among insects has been in existence for minimally 165 Mya.
81 This ancient association also will provide new insight for exploring the predator–prey relationships
82 among insects and lichens, and the role of habitat during mid-Mesozoic time.

83

84 **Results**

85 **Reanalysis of the previously suspected lichen fossil *Daohugouthallus ciliiferus***

86 We have studied five fossil lichen specimens, PB23120, B0474, B0476P/C,
87 CNU-LICHEN-NN2019001 and CNU-LICHEN-NN2019002P/C, all of which were collected from the
88 Daohugou 1 locality of Inner Mongolia. The newly collected specimens were identified to be
89 *Daohugouthallus ciliiferus* based on careful observations of its distinctive morphology.

90

91 **Genus** *Daohugouthallus* Wang, Krings *et* Taylor, 2010

92 **Species** *Daohugouthallus ciliiferus* Wang, Krings *et* Taylor, 2010

93

94 **Emended diagnosis.** The diagnosis is as follows and adds to the previous assessment (*Wang X et al.,*

95 2010). Thallus foliose to subfruticose; lobes ca. 20–30 mm long, irregularly branched, margin
96 sometimes revolute; lateral and terminal branches ca. 0.5–5.0 mm long, tips tapered; upper surface
97 smooth, partly broken; aggregated black spots often present, punctiform; cilia sometimes present near
98 the branch tips, forming filiform appendages; lobules occasionally present (*Figure 1*).

99 Besides the external morphology, certain anatomic characters also were determined. Upper cortex
100 conglutinate, comprising one cell layer, very thin, ca. 1 µm thick (*Figure 2A*); algal cells globose to
101 near globose, one-celled, mostly 1.5–2.1 µm in diameter, some in framboidal form, interconnected
102 (*Figure 2A, B, F*) by or adhered (*Figure 2C, D, E–G, H*) to the fungal hyphae with simple wall-to-wall
103 mycobiont-photobiont interface; fungal hyphae filamentous, some shriveled, septate (*Figure 2B, C, G,*
104 *H*), 1.2–1.5 µm wide. These additional features (*Figure 2*) support the above diagnoses that this
105 specimen is a fossil lichen.

106 **Remarks.** This adpression lichen fossil was reported by Wang X *et al.* (2010) as a new genus and new
107 species of lichen, i.e. *Daohugouthallus ciliiferus*. However, there were no anatomic characters
108 including both fungal and algal components that was provided and consequently its lichen affinity was
109 doubted and thought as ambiguous (*Honegger et al., 2013; Lücking and Nelsen, 2018*). Actually, the
110 lichen fossil now has been well defined and should accord with three important criteria: presence of a
111 mycobiont component, presence of a photobiont component, and presence of spatial connections
112 between both components (*Lücking and Nelsen, 2018*). Accordingly, thallus sections were made in this
113 study and relevant anatomic details can be observed. First, the upper cortex occasionally was present
114 (*Figure 2A*), and the septa of fungal hyphae also is documented (*Figure 2C, D*). Second, the algal cells
115 are globose and occasionally have a spherical assembly of microcrystals in framboidal form similar to
116 *Trebouxia* of *Chlorolichenomycites salopenis* in morphology but much smaller (*Honegger et al.,*

117 2013). Third, the spatial connections between fungal hyphae and algal cells have been observed, mostly
118 consisting of fungal hyphae interweaved with algal cells (*Figure 2A, C, D, F*). The above-mentioned
119 characters of *Daohugouthallus ciliiferus* accords well with the definition of lichen fossil and indicate a
120 strong affinity to a lichen. From the external morphology, *Daohugouthallus ciliiferus* would be easily
121 associated with extant *Everniastrum cirrhatum*, a conclusion that requires further study in the near
122 future.

123

124 **Systematic Paleontology**

125 The lichen-mimicking insects represent a new genus and two new species affiliated to Ithonidae of the
126 order Neuroptera. The terminology of venation follows Breitkreuz *et al.* (2017).

127

128 **Order** Neuroptera Linnaeus, 1758

129 **Family** Ithonidae Newman, 1853 *sensu* Winterton *et* Makarkin, 2010

130 **Genus** *Lichenipolystoechotes* Fang, Zheng *et* Wang, gen. nov.

131

132 **Included species.** *Lichenipolystoechotes angustimaculatus* Fang, Zheng *et* Wang, sp. nov. (type
133 species), *Lichenipolystoechotes ramimaculatus* Fang, Ma *et* Wang, sp. nov.

134 **Etymology.** The new genus name is a combination of *lichen* and *Polystoechotes* (a genus name of
135 Ithonidae) in reference to the lichen-mimesis of the genus. The gender is masculine.

136 **Diagnosis.** Forewing ellipsoidal shaped, medium length, slightly narrow with length-width ratio 3.25–
137 3.5; membrane bearing coralliform pattern with unclosed diaphanous U-shaped fenestrae along the
138 margin in forewing; costal space slightly broad basally, then narrowed towards wing apex; ScA and

139 recurved humeral veinlet present; costal cross-veins simple in proximal half, and then distally forked;
140 ScP and RA fused distally, ending close to the wing apex, no cross-veins present in this area;
141 cross-veins in area between RA and RP scattered; RP with about 18 branches, RP1 a single branch, few
142 cross-veins scattered at the radial sector; M forked beyond the separation point of RP1, MA and MP
143 with the similar branched pattern, the number of MP branches slightly more than MA; CuA distinctly
144 multi-forked, with 7–10 pectinate branches; CuP bifurcated.

145 **Remarks.** The new genus can easily be assigned to Ithonidae by the following characters: medium
146 body size, prolonged forewing, relatively narrow costal space, and presence of ScA and recurrent
147 humeral veinlet. In addition, its forewing characters, including Sc and R1 fused distally, few
148 cross-veins except for a row of well-defined outer gradate series in radial sector, MP forked beyond
149 MA divergence, conforming to a polystoechotid affiliation (Zheng *et al.*, 2016). It also is distinguished
150 from other polystoechotid genera by the distinctive coralliform markings of the forewings.

151

152 ***Lichenipolystoechotes angustimaculatus* Fang, Zheng et Wang, sp. nov.** (Figures 3A–D, 4E)

153 **Etymology.** The specific name comes from the Latin words “*angusta*” and “*macula*” referring,
154 respectively, to the narrow, linear and pigmented swaths on the forewing, and the spot-like patterns
155 present on those swaths.

156 **Material.** *Holotype.* CNU-NEU-NN2016040P/C (Figures 3A–C, 4E), *paratype.*

157 CNU-NEU-NN2016041 (Figure 3D).

158 **Type locality and horizon.** Daohugou 1, near Daohugou Village, Shantou Township, Ningcheng
159 County, Inner Mongolia, China. Jiulongshan Formation, Callovian–Oxfordian boundary interval, latest
160 Middle Jurassic.

161 **Diagnosis.** Forewing, humeral veinlet strongly recurved; ScA present; cross-veins in area between RA
162 and RP scattered except for the middle gradate series; RP with about 18 branches; MA and MP with
163 similarly distal pectinate branches; CuA pectinately branched in distal half; CuP deeply bifurcated at
164 anterior half.

165 **Description and comparison.** Only forewing present. Forewing elongate, oval shaped, about 21.3 mm
166 long, 6.5 mm wide; membrane bearing irregular coralloid markings of pigmentation, forming many
167 diaphanous marginal fenestrae; costal space slightly broad basally, then narrowed towards the wing
168 apex; costal cross-veins scarcely branched in proximal half of wing, and then forming bifurcated
169 branches in distal half; sc-ra cross-vein absent; space between RA and RP relatively narrow with seven
170 cross-veins; RP with 18 pectinate branches, and each branch bifurcated near wing margin; cross-veins
171 in radial sector relatively scarce except for the middle gradate series; M forked slightly beyond the
172 separation of RP1; MA and MP forming 7 pectinate branches each; CuA pectinate branched in distal
173 half part, forming 7 pectinate branches; CuP first bifurcated at the proximal half, then forming the
174 distal simple forks; A1–A3 forming several pectinate branches; a few cross-veins present among MA
175 and A3.

176

177 ***Lichenipolystoechotes ramimaculatus* Fang, Ma et Wang, sp. nov.** (Figures 3E–H, 4A, G)

178 **Etymology.** The specific name comes from the Latin word *rami* and *macula*, referring, respectively, to
179 the narrow, branched and pigmented swaths traversing the forewing, and the spot-like patterns present
180 on those branched swaths.

181 **Material.** Holotype. CNU-NEU-NN2019006P/C (Figures 3E–H, 4A, G).

182 **Type locality and horizon.** Daohugou 1, near Daohugou Village, Shantou Township, Ningcheng

183 County, Inner Mongolia, China. Jiulongshan Formation, Callovian–Oxfordian boundary interval, latest
184 Middle Jurassic.

185 **Diagnosis.** The marginal diaphanous fenestrae significantly open, surrounded by pigmented zones; MA
186 forming the distal dichotomizing fork, MP with 6 pectinate distal branches; CuA branched nearly at the
187 middle, forming about 11 pectinate branches, CuP bifurcated beyond the middle portion of the vein.

188 **Description and Comparison.** Only forewing preserved. Forewing elongate, oval shaped, about 22.8
189 mm long, 6.5 mm wide; costal space slightly broadened, then narrowed towards wing apex; subcostal
190 veinlets relatively widely spaced, scarcely branched medially, forming multiple bifurcated branches
191 distally; areas between Sc and RA narrow, without crossveins; space between RA and RP relatively
192 narrow with sparse crossveins; RP with about 22 pectinate branches; RP1 branched from RP near wing
193 base, single until wing margin; M forked basally, MA forming 2 distal dichotomous branches, and MP
194 forming 6 distal pectinate branches; CuA pectinate medially to distally, forming 11 pectinate branches;
195 CuP bifurcated at middle; A1–A3 partly preserved.

196

197 **Discussion**

198 The two new species of *Lichenipolystoechotes* exhibit a very similar appearance, but they easily can be
199 separated by the distinct differences of branches of the MA and CuA veins. *Lichenipolystoechotes*
200 species are conspicuous based on their highly prominent, homologous, pigmentation pattern of their
201 forewings, which implies that these insects evolved a similar defensive strategy. The closest extant
202 relatives of *Lichenipolystoechotes* are Ithonidae (moth lacewings), of which their ecological and
203 biological features are poorly documented (New, 1989). The forewings of the two new species
204 demonstrate a high similarity in their overall appearance, such as the forewing branching pattern

205 (*Figure 3A, E, 4A*) that matches the thallus branches of the co-occurring foliose to subfruticose lichen
206 *Daohugouthallus ciliiferus* (*Figure 4B–D*) (*Wang X et al., 2010*). The entire forewing forms an
207 irregular branching pattern amid rounded, diaphanous fenestrae (windows) that are distributed along
208 the wing center and as U-shaped extensions occurring around the wing border. The pigmented branch
209 pattern of the wings has uneven widths and is angulated outwardly. The variation in width of each
210 forewing vein branch conforms well to the variation in width of the lichen's branches, indicating a
211 morphological similarity between the wing markings and lichen thallus (*Figure 4F; Figure 4–figure*
212 *supplement 1; Supplementary file 1: Table S1*). Lichens often have punctiform pycnidia (asexual
213 reproductive structures) with black spots appearing on their thallus, especially in extant foliose lichen
214 families such as Parmeliaceae (*Thell et al., 2012*). In *Daohugouthallus ciliiferus* specimens, punctiform
215 black spots occur, but whether they are pycnidia is uncertain. It is noteworthy that a specimen of *L.*
216 *ramimaculatus* displays similar, scattered spots on its wings that resemble the dark spots on the lichen
217 thallus of *D. ciliiferus* (*Figure 4G–I*), potentially strengthening the similarity between *L.*
218 *ramimaculatus* and *D. ciliiferus*. Collectively, these details of insect morphology likely enhanced the
219 similarity of the insect with a co-occurring lichen, providing a reasonable inference that the forewing is
220 mimetic with the lichen thallus.

221 It is generally known that lichens are stable, symbiotic associations of fungi and algae (*Lücking*
222 *and Nelsen, 2018*). At the same time, lichens are regarded as pioneers in the colonization of novel
223 surfaces such as bark, rock and soil, which dominate about 7% of the earth's terrestrial surface (*Larson,*
224 *1987*), and have a distribution from the polar regions to the tropics (*Lumbsch and Rikkinen, 2017*).
225 They are prominent in arctic-alpine vegetation types in wet and higher montane forests (*Lumbsch and*
226 *Rikkinen, 2017*). Many extant foliose or fruticose lichens such as taxa of Parmeliaceae are known to be

227 epiphytic or corticolous, and bark surfaces are one of the most common substrates (*Lumbsch and*
228 *Rikkinen, 2017*). *Daohugouthallus ciliiferus* is considered an epiphytic foliose to subfruticose lichen,
229 and often is found entangled with gymnosperm seed cones (*Figure 1C, 4D*) (*Wang X et al., 2010*).
230 When *Lichenipolystoechotes* moth lacewings reposed in a habitat rich in *D. ciliiferus*, a near perfect
231 match of their appearances would assist their concealment. Among extant Neuroptera, similar
232 appearances of lichen-camouflage or related cases have been recorded in some larvae of green
233 lacewings that carry packets of lichen material on their backs to hide themselves (*Slocum and Lawrey,*
234 *1976; Wilson and Methven, 1997*). Although *Lichenipolystoechotes* probably lacked the same life-habit
235 as modern lichen-carrying chrysopoid larvae, the Jurassic taxa likely acquired a similar survival
236 advantage when they occupied a lichen-rich habitat. Some extant *Thyridosmylus* species of Osmylidae,
237 another archaic lineage of Neuroptera, possess similar complex wing markings and often occur on
238 moss-laden surfaces of rocks, tree bark and indurated soil surfaces (*Winterton et al., 2017: fig. 2B*),
239 which exhibit an impressive consistency with their surroundings (pers. observ. by Yongjie Wang).
240 Although *Lichenipolystoechotes* is a member of Ithonidae, phylogenetically distant to Osmylidae, we
241 infer that their concealment strategy of mimicking cryptogam plants in certain habitats has a deep
242 geochronologic history among ancient lacewing lineages.

243 Unlike the models of other, co-occurring, plant-mimicking insects, lichen-mimesis of
244 *Lichenipolystoechotes* appears highly specialized (*Figure 5*). Modern lichens can produce a variety of
245 lichenic acids (*Gerson, 1973*) that are unpalatable to many insects and enhance the protective sheltering
246 for animals. Consequently, lichens and lichen-tolerant animals, such as lichen feeding insects and mites,
247 constitute a unique micro-ecosystem. We hypothesize that such a micro-ecosystem existed 165
248 million-years-ago in Northeastern China that accommodated these trophic, sheltering, defensive and

249 mimetic interactions. Although lichen mimesis is not well documented among extant insects, the most
250 iconic such case of lichen and insect resemblance is the industrial melanism of the peppered moth
251 *Biston betularia* in nineteenth century Britain (*Gerson, 1973; Stevens and Merilaita, 2011*). The
252 Industrial Revolution caused elevated levels of soot laden air pollution that resulted in disappearance of
253 lichen shelters for the light-colored morph of *B. betularia*, as their corresponding habitation sites were
254 changed from lightly tinged to dark-hued lichen surfaces that led to their greater vulnerability to
255 predation. This change resulted in the abrupt increase of the dark colored morph of *B. betularia*. When
256 lightly hued lichens returned after aerial pollution was thwarted, *B. betularia* again became dominant
257 as the lightly colored morph. The industrial melanism of *B. betularia* was believed as a textbook
258 example of Darwinian evolution in action, though it was questioned by some authors (*Sargent, 1968,*
259 *1969; Coyne, 1998; Cook and Saccheri, 2013*). Nevertheless, other studies demonstrated that selection
260 pressures such as predation by birds genuinely affected the differential survival of the pale and dark
261 colored morphs of *B. betularia* under differently hued backgrounds (*Howlett and Majerus, 1987;*
262 *Liebert and Brakefield, 1987; Majerus, 2009; Walton and Stevens, 2018*). It is possible that the Jurassic
263 *Lichenipolystoechotes* could have gained survival advantage from mimesis of a lichen similar to that of
264 modern *B. betularia*–lichen mimesis. Specifically, if lichen models were present in the habitat occupied
265 by *Lichenipolystoechotes*, survival of the mimic would be assured. It is noteworthy that the winged
266 adults of *Lichenipolystoechotes* would not have been always in the shelter of a lichen model; however,
267 when they were, the conditions of mating, laying of eggs and dispersal would be paramount for
268 survival. If so, high-contrast lichen-like markings could contribute to concealment of the insects.
269 Alternatively, such high-contrast markings of *Lichenipolystoechotes* species also can be interpreted as
270 disruptive coloration, which would confuse the boundaries of moth lacewing and lichen to prevent the

271 detection of a body part essential for survival (*Stevens and Merilaita, 2011*). Consequently, the
272 lichen-like markings of *Lichenipolystoechotes* could likely bring the double protections to the
273 insects-background mimicry and disruptive coloration.

274 Was there possible benefit to *D. ciliiferus* from its mimetic association with *Lichenipolystoechotes*?

275 This is an open question that could raise multiple alternative explanations. Some modern insects such
276 as ants, dipterans and larva of green lacewings are considered to potentially contribute to dispersal of
277 lichens by transporting lichen propagules to new sites of colonization (*Gerson, 1973; Keller and*
278 *Scheidegger, 2016; Ronnås et al., 2017*). In a comparison with such relatively small, lichen-carrying
279 insects, *Lichenipolystoechotes* possessed a considerably larger body size that likely was convenient for
280 dispersal of lichen propagules. Notably, sexual reproductive organs such as apothecia have not been
281 found on the *D. ciliiferus* thallus based on light-microscopic morphological and SEM anatomical
282 observations; neither were vegetative propagules such as soredia or isidia seen except along marginal
283 lobules that occasionally were present. This hypothesis of zoochory requires additional evidence for
284 support. However, our alternative hypothesis of benefiting *D. ciliiferus* is based on trophic interactions.
285 As predaceous insects, *Lichenipolystoechotes* inhabited a lichen-rich environment to evade their
286 predators, but they also could have predated and consumed smaller lichen-feeding animals while
287 simultaneously decreasing herbivore damage to the *D. ciliiferus* thallus. This latter hypothesis would
288 require additional verification from evidence of a small ecological web of predator, shelter, defensive
289 and mimetic interactions associated with *Daohugouthallus* and *Lichenipolystoechotes* in the same
290 deposit.

291 The accepted oldest lichen fossil was reported from the Early Devonian and lichens have existed
292 minimally for 410 million years (*Taylor et al., 1995; Honegger et al., 2013; Lücking and Nelsen, 2018*),

293 as have the apterygote insects (*Misof et al., 2014*). Both archaic Devonian lineages have evolved more
294 derived, diverse clades of lichens and pterygote insects resulting in a myriad of associations among
295 their modern lineages (*Figure 6*). Although there is virtually no evidence to suggest when and how
296 such associations began; in this report, we describe the oldest examples of lichen mimesis that involved
297 two lacewing species resembling a contemporaneous lichen from the same, latest Middle Jurassic
298 deposit. These insect lineages have acquired mimicry associations with lichens in less than half of the
299 time (40 %) of the duration of both major lineages since the early Devonian (*Figure 6*). This new
300 finding documents a unique survival strategy among mid-Mesozoic Neuroptera, and others await
301 discovery.

302

303 **Materials and methods**

304 **Geological Context.** Specimens were collected from the Daohugou 1 locality of the Jiulongshan
305 Formation, near Daohugou Village, Ningcheng County, approximately 80 km south of Chifeng City, in
306 the Inner Mongolia Autonomous Region, China (119°14.318'E, 41°18.979'N). The age of this
307 formation is 168–152 Ma based on $^{40}\text{Ar}/^{39}\text{Ar}$ and $^{206}\text{Pb}/^{238}\text{U}$ isotopic analyses (*He et al., 2004; Liu et*
308 *al., 2006; Ren, 2019*).

309 **Specimen Repository.** CNU-NEU-NN2016040P/C and CNU-NEU-NN2016041 of
310 *Lichenipolystoechotes angustimaculatus* sp. nov., and CNU-NEU-NN2019004P/C of
311 *Lichenipolystoechotes ramimaculatus* sp. nov. are housed in the College of Life Sciences and Academy
312 for Multidisciplinary Studies, Capital Normal University (CNU), Beijing, China. Lichen specimens of
313 *Daohugouthallus ciliiferus* Wang, Krings *et Taylor*, 2010: PB23120 is housed in the paleobotanical
314 collection of the Nanjing Institute of Geology and Palaeontology, Chinese Academy of Sciences, in

315 Nanjing, China; B0474 and B0476P/C are housed in the Institute of Vertebrate Paleontology and
316 Paleanthropology, Chinese Academy of Sciences, in Beijing, China; CNU-LICHEN-NN2019001 and
317 CNU-LICHEN-NN2019002P/C are housed in the Key Lab of Insect Evolution and Environmental
318 Changes, College of Life Sciences and Academy for Multidisciplinary Studies, Capital Normal
319 University, in Beijing, China.

320 ***Experimental Methods.*** The insect and lichen fossils were examined and photographed using a Nikon
321 SMZ25 microscope attached to a Nikon DS-Ri2 digital camera system at the Key Lab of Insect
322 Evolution and Environmental Changes at Capital Normal University in Beijing, China. Lichen
323 compression specimens from the Daohugou 1 locality were soaked in water for several seconds, dried
324 on filter paper, and then a fragment was lifted up by the edge of a razor blade. One isolated, dried slice
325 was examined and photographed using a Zeiss Axioscope2 compound microscope attached to a Nikon
326 D5100 digital camera system at the State Key Laboratory of Mycology, Institute of Microbiology, at
327 the Chinese Academy of Sciences in Beijing. That piece of lichen fossil then was sputter-coated with
328 gold particles using an Ion Sputter E-1045 (HITACHI), and SEM images were recorded using a
329 scanning electron microscope (Hitachi SU8010) with a secondary electron detector operated at 5.0 kV.
330 Overlay drawings were prepared by Corel DRAW. Box plots were made with Origin 2018 software,
331 which is used to display the distribution of the data of branch width of *L. ramimaculatus*'s forewing
332 pattern and lichen thallus of *D. ciliiferus*. The box plots are formed by two quartiles showing the high
333 frequency of values, and the upper and lower points of the boxes are the maximum and minimum
334 values. All figures were composited in Adobe Photoshop.

335 **Acknowledgements**

336 We sincerely thank Dr. George Perry (Editor), Dr. Robert Lücking (Reviewer), Dr. Enrique Peñalver

337 (Reviewer), and another anonymous reviewer for their critical comments and constructive suggestions
338 to improve this paper. We are grateful to Dr. Chong Dong (Nanjing Institute of Geology and
339 Palaeontology, Chinese Academy of Sciences) for providing Figure 4C and Dr. Boyang Sun (Institute
340 of Vertebrate Paleontology and Paleoanthropology, Chinese Academy of Sciences) for assisting the
341 loan of lichen specimens B0474 and B0476P/C. We thank Xiaoran Zuo for drawing the habitus
342 reconstruction picture in Figure 5. We also thank Xuedong Li (College of Life Sciences and Academy
343 for Multidisciplinary Studies, Capital Normal University) for assisting us in the analysis of fossil
344 lichens. This report is contribution 382 of the Evolution of Terrestrial Ecosystems at the National
345 Museum of Natural History in Washington, D.C.

346

347 **References**

- 348 Badano D, Engel MS, Basso A, Wang B, Cerretti P. 2018. Diverse Cretaceous larvae reveal the
349 evolutionary and behavioural history of antlions and lacewings. *Nature Communications* **9**:1–14.
350 DOI: <https://doi.org/10.1038/s41467-018-05484-y>
- 351 Braun H. 2011. The little lichen dragon – an extraordinary katydid from the Ecuadorian Andes
352 (Orthoptera, Tettigoniidae, Phaneropterinae, Dysoniini). *Zootaxa* **3032**:33–39. DOI:
353 <https://doi.org/10.11646/zootaxa.3032.1.3>
- 354 Breitzkreuz LCV, Winterton SL, Engel MS. 2017. Wing tracheation in Chrysopidae and other
355 Neuroptera (Insecta): a resolution of the confusion about vein fusion. *American Museum Novitates*
356 **3890**:1–44. DOI: <https://doi.org/10.1206/3890.1>
- 357 Capinera JL. (ed). 2008. *Encyclopedia of entomology*. Springer Science & Business Media.
- 358 Cannon P, 2010. Lichen camouflage and lichen mimicry. *British Lichen Society Bulletin* **106**:39–41.

359 Cook LM, Saccheri IJ. 2013. The peppered moth and industrial melanism: evolution of a natural
360 selection case study. *Heredity* **110**:207–212. DOI: <https://doi.org/10.1038/hdy.2012.92>

361 Coyne JA. 1998. Not black and white. *Nature* **396**:35–36. DOI: <https://doi.org/10.1038/23856>

362 Garrouste R, Hugel S, Jacquelin L, Rostan P, Steyer JS, Desutter-Grandcolas L, Nel A. 2016. Insect
363 mimicry of plants dates back to the Permian. *Nature Communications* **7**:1–6. DOI:
364 <https://doi.org/10.1038/ncomms13735>

365 Gerson U. 1973. Lichen–arthropod Associations. *Lichenologist* **5**:434–443. DOI:
366 <https://doi.org/10.1017/S0024282973000484>

367 Gullan, PJ, Cranston PS. 2014. *The insects: an outline of entomology*. John Wiley & Sons.

368 He HY, Wang XL, Zhou ZH, Zhu RX, Jin F, Wang F, Ding X, Boven A. 2004. ⁴⁰Ar/³⁹Ar dating of
369 ignimbrite from Inner Mongolia, Northeastern China, indicates a post-Middle Jurassic age for the
370 overlying Daohugou bed. *Geophysical Research Letters* **31**:1–4. DOI:
371 <https://doi.org/10.1029/2004GL020792>

372 Honegger R, Edwards D, Axe L. 2013. The earliest records of internally stratified cyanobacterial and
373 algal lichens from the Lower Devonian of the Welsh Borderland. *New Phytologist* **197**:264–275.
374 DOI: <https://doi.org/10.1111/nph.1200>

375 Howlett RJ, Majerus ME. 1987. The understanding of industrial melanism in the peppered moth
376 (*Biston betularia*) (Lepidoptera: Geometridae). *Biological Journal of the Linnean Society* **30**:31–
377 44. DOI: <https://doi.org/10.1111/j.1095-8312.1987.tb00286.x>

378 Keller C, Scheidegger C. 2016. Multiple mating events and spermatia-mediated gene flow in the
379 lichen-forming fungus *Lobaria pulmonaria*. *Herzogia* **29**:435–450. DOI:
380 <https://doi.org/10.13158/heia.29.2.2016.435>

381 Larson DW. 1987. The absorption and release of water by lichens. *Bibliotheca Lichenologica* **25**:351–
382 360.

383 Liebert TG, Brakefield PM. 1987. Behavioural studies on the peppered moth *Biston betularia* and a
384 discussion of the role of pollution and lichens in industrial melanism. *Biological Journal of the*
385 *Linnean Society* **31**:129–150. DOI: <https://doi.org/10.1111/j.1095-8312.1987.tb01985.x>

386 Liu XY, Shi GL, Xia FY, Lu XM, Wang B, Engel MS. 2018. Liverwort mimesis in a Cretaceous
387 lacewing larva. *Current Biology* **28**:1475–1481. DOI: <https://doi.org/10.1016/j.cub.2018.03.060>

388 Liu YX, Liu YQ, Zhong H. 2006. LA-ICPMS zircon U-Pb dating in the Jurassic Daohugou beds and
389 correlative strata in Ningcheng of Inner Mongolia. *Acta Geologica Sinica-English Edition* **80**:733–
390 742. DOI: <https://doi.org/10.1111/j.1755-6724.2006.tb00296.x>

391 Lücking R. 2001. Lichens on leaves in tropical rainforests: life in a permanently ephemeral
392 environment. *Dissertationes Botanicae* **346**:41–77.

393 Lücking R, Mata-Lorenzen J, Dauphin LG. 2010. Epizoic liverworts, lichens and fungi growing on
394 Costa Rican shield mantis (Mantodea: *Choeradodis*). *Studies on Neotropical Fauna and*
395 *Environment* **45**:175–186. DOI: <https://doi.org/10.1080/01650521.2010.532387>

396 Lücking R, Nelsen MP. 2018. Ediacarans, protolichens, and lichen-derived *Penicillium*: a critical
397 reassessment of the evolution of lichenization in fungi. In: Krings M, Harper CJ, Cuneo NR,
398 Rothwell GW (eds). *Transformative paleobotany*. Academic Press, pp 551–590. DOI:
399 <https://doi.org/10.1016/B978-0-12-813012-4.00023-1>

400 Lumbsch H, Rikkinen J. 2017. Evolution of lichens. In: Dighton J, White J (eds). *The fungal*
401 *community: its organization and role in the ecosystem*. Boca Raton, CRC Press, pp 53–62. DOI:
402 <https://doi.org/10.1201/9781315119496-5>

403 Majerus MEN. 2009. Industrial melanism in the peppered moth, *Biston betularia*: an excellent teaching
404 example of darwinian evolution in action. *Evolution: Education and Outreach* **2**:63–74. DOI:
405 <https://doi.org/10.1007/s12052-008-0107-y>

406 Maran T. 2017. *Mimicry and meaning: Structure and semiotics of biological mimicry. Vol. 16*. Berlin:
407 Springer.

408 Misof B. et al. 2014. Phylogenomics resolves the timing and pattern of insect evolution. *Science*
409 **346**:763–767. DOI: <https://doi.org/10.1126/science.1257570>

410 New TR. 1989. Lacewings. In: Fischer M (ed). *Handbook of Zoology. Volume IV Arthropoda: Insecta*.
411 Berlin: Walter de Gruyter.

412 Pérez-de la Fuente R, Delclòs X, Peñalver E, Speranza M, Wierzos J, Ascaso C, Engel MS. 2012.
413 Early evolution and ecology of camouflage in insects. *Proceedings of the National Academy of*
414 *Sciences of the United States of America* **190**:21414–21419. DOI:
415 <https://doi.org/10.1073/pnas.1213775110>

416 Pérez-de la Fuente R, Peñalver E, Azar D, Engel MS. 2018. A soil-carrying lacewing larva in Early
417 Cretaceous Lebanese amber. *Scientific Reports* **8**:1–12. DOI:
418 <https://doi.org/10.1038/s41598-018-34870-1>

419 Ronnås C, Werth S, Ovaskainen O, Varkonyi G, Scheidegger C, Snäll T. 2017. Discovery of
420 long-distance gamete dispersal in a lichen-forming ascomycete. *New Phytologist* **216**:216–226. DOI:
421 <https://doi.org/10.1111/nph.14714>

422 Ren D. 2019. Jurassic-Cretaceous non-marine stratigraphy and entomofaunas in Northern China. In:
423 Ren D, Shih CK, Gao TP, Wang YJ, Yao YZ (eds). *Rhythms of Insect Evolution*. Wiley. pp 1–16.
424 DOI: <https://doi.org/10.1002/9781119427957>

425 Sargent TD. 1968. Cryptic moths: effects on background selections of painting the circumocular scales.
426 *Science* **159**:100–101. DOI: <https://doi.org/10.1126/science.159.3810.100>

427 Sargent TD. 1969. Background selections of the pale and melanic forms of the cryptic moth. *Phigalia*
428 *titea* (Cramer). *Nature* **222**:585–586. DOI: <https://doi.org/10.1038/222585b0>

429 Skorepa AC, Sharp AJ. 1971. Lichens in 'packets' of lacewing larvae (Chrysopidae). *Bryologist*
430 **74**:363–364. DOI: <https://doi.org/10.2307/3241643>

431 Slocum RD, Lawrey JD. 1976. Viability of the epizoic lichen flora carried and dispersed by green
432 lacewing (*Nodita pavidata*) larvae. *Canadian Journal of Botany* **54**:1827–1831. DOI:
433 <https://doi.org/10.1139/b76-196>

434 Stevens M, Merilaita S. (eds) 2011. *Animal camouflage: mechanisms and function*. Cambridge
435 University Press.

436 Tauber CA, Tauber MJ, Albuquerque GS. 2014. Debris-carrying in larval Chrysopidae: unraveling its
437 evolutionary history. *Annals of the Entomological Society of America* **107**:295–314. DOI:
438 <https://doi.org/10.1603/AN13163>

439 Taylor TN, Hass H, Remy W, Kerp H. 1995. The oldest fossil lichen. *Nature* **378**:244–244. DOI:
440 <https://doi.org/10.1038/378244a0>

441 Thell A, Crespo A, Divakar PK, Kärnefelt I, Leavitt SD, Lumbsch HT, Seaward MRD. 2012. A review
442 of the lichen family Parmeliaceae – history, phylogeny and current taxonomy. *Nordic Journal of*
443 *Botany* **30**:641–664. DOI: <https://doi.org/10.1111/j.1756-1051.2012.00008.x>

444 Walton OC, Stevens M. 2018. Avian vision models and field experiments determine the survival value
445 of peppered moth camouflage. *Communications Biology* **1**:1–7. DOI:
446 <https://doi.org/10.1038/s42003-018-0126-3>

447 Wang B, Xia FY, Engel MS, Perrichot V, Shi GL, Zhang HC, Chen J, Jarzembowski EA, Wappler T,
448 Rust J. 2016. Debris-carrying camouflage among diverse lineages of Cretaceous insects. *Science*
449 *Advances* **2**:e1501918. DOI: <https://doi.org/10.1126/sciadv.1501918>

450 Wang M, Béthoux O, Bradler S, Jacques FMB, Cui YY, Ren D. 2014. Under cover at pre-angiosperm
451 times: a cloaked phasmatodean insect from the Early Cretaceous Jehol biota. *PLoS One* **9**:e91290.
452 DOI: <https://doi.org/10.1371/journal.pone.0091290>

453 Wang X, Krings M, Taylor NT. 2010. A thalloid organism with possible lichen affinity from the
454 Jurassic of northeastern China. *Review of Palaeobotany and Palynology* **162**:591–598. DOI:
455 <https://doi.org/10.1016/j.revpalbo.2010.07.005>

456 Wang YJ, Labandeira CC, Shih CK, Ding QL, Wang C, Zhao YY, Ren D. 2012. Jurassic mimicry
457 between a hangingfly and a ginkgo from China. *Proceedings of the National Academy of Sciences*
458 *of the United States of America* **109**:20514–20519. DOI: <https://doi.org/10.1073/pnas.1205517109>

459 Wang YJ, Liu ZQ, Wang X, Shih CK, Zhao YY, Engel MS, Ren D. 2010. Ancient pinnate leaf mimesis
460 among lacewings. *Proceedings of the National Academy of Sciences of the United States of*
461 *America* **107**:16212–16215. DOI: <https://doi.org/10.1073/pnas.1006460107>

462 Wilson PJ, Methven AS. 1997. Lichen use by larval *Leucochrysa pavid*a (Neuroptera: Chrysopidae).
463 *Bryologist* **100**:448–453. DOI: <https://doi.org/10.2307/3244405>

464 Winterton SL, Zhao J, Garzón-Orduña IJ, Wang YJ, Liu ZQ. 2017. The phylogeny of lance lacewings
465 (Neuroptera: Osmylidae). *Systematic Entomology* **42**:555–574. DOI:
466 <https://doi.org/10.1111/syen.12231>

467 Yang HR, Shi CF, Engel MS, Zhao ZP, Ren D, Gao TP. 2020. Early specializations for mimicry and
468 defense in a Jurassic stick insect. *National Science Review* DOI:

469 <https://doi.org/10.1093/nsr/nwaa056>

470 Zheng B, Ren D, Wang Y. 2016. Earliest true moth lacewing from the Middle Jurassic of Inner

471 Mongolia, China. *Acta Palaeontologica Polonica* **61**:847–851. DOI:

472 <https://doi.org/10.4202/app.00259.2016>

473

474

475 **Figure captions**

476 **Figure 1.** Photos of the lichen *Daohugouthallus ciliiferus* Wang, Krings *et* Taylor, 2010. (A) Specimen
477 B0476P, with arrows indicating the lobules. (B) Specimen CNU-LICHEN-NN2019001, with arrows
478 indicating the lobules. (C) Specimen CNU-LICHEN-NN2019002P. Scale bars: 5 mm in A–C.

479

480 **Figure 2.** Scanning electron microscopy (SEM) micrographs of lichen fossil
481 (CNU-LICHEN-NN2019001). (A) Thallus longitudinal section containing the cortex, with white
482 arrows pointing to the fungal hyphae, and black ones to the algal cells. The fungal hyphae are
483 interweaved with algal cells. (B–D, F–H) Fungal hyphae indicated by white arrows; algal cells are
484 indicated by black arrows showing entanglement and encirclement by fungal hyphae; septa shown in B,
485 C, G, H. (E) One algal cell indicated by the black arrow, displaying adherence to other fungal hyphae
486 indicated by the white arrow. Scale bars: 5 μ m in A, C, D, G, H; 10 μ m in B; 3 μ m in E; 4 μ m in F.

487

488 **Figure 3.** Photos and line drawings of *Lichenipolystoechotes angustimaculatus* gen. *et* sp. nov., and *L.*
489 *ramimaculatus* gen. *et* sp. nov. (A–C) Holotype CNU-NEU-NN2016040P/C of *L. angustimaculatus*,
490 photo of part in (A). Accompanying overlay drawing in (B). Photo of counterpart in (C). (D) Photo of
491 the paratype CNU-NEU-NN2016041 of *L. angustimaculatus*. (E–H) The holotype
492 CNU-NEU-NN2019006P/C of *L. ramimaculatus*, with a lichen mimicking forewing pattern. Photo of
493 part in (E); accompanying overlay drawing in (F); photo of counterpart in (G); and accompanying
494 overlay drawing in (H). Scale bars: 5 mm in A–H.

495

496 **Figure 4.** The lichen mimicking lacewing *Lichenipolystoechotes ramimaculatus* gen. *et* sp. nov. and *L.*

497 *angustimaculatus* gen. et sp. nov., and fossils of the contemporaneous lichen *Daohugouthallus*
498 *ciliiferus* Wang, Krings et Taylor, 2010. (A) Photo of part of *L. ramimaculatus*, with a lichen
499 mimicking forewing pattern, CNU-NEU-NN2019004P. (B–C) Photos of the lichen thallus *D. ciliiferus*,
500 PB23120; thallus segment in (B); and entire thallus in (C). Photos A–C are at the same scale. (D) Photo
501 of a nearly intact lichen thallus of *D. ciliiferus*, B0474. (E) Photo of *L. angustimaculatus* with a lichen
502 mimicking wing pattern; CNU-NEU-NN2016040P. (F) Box scatter plots of measurement data
503 displaying lower and upper extremes, lower and upper quartile, median and average (in the blue dotted
504 line) of branch widths of *L. ramimaculatus*'s forewing pattern (CNU-NEU-NN2019004C) and thallus
505 branch widths of lichen *D. ciliiferus* (PB23120, B0474) separately. (Black, red and green dots represent
506 measurement results of branch pattern widths of lichen-mimicking lacewing and thallus widths of the
507 two lichen specimens, respectively.) (G) Part of the wing pattern of *L. ramimaculatus*, with irregular
508 wing spots. (H, I) Portion of the thallus of *D. ciliiferus*, with irregular spot-like punctiform pycnidia,
509 B0474 (H), B0476P (I) The dark arrows indicate the spots on wing of *L. ramimaculatus* and thallus of
510 *D. ciliiferus*. Scale bars: 5 mm in A–E, 1 mm in G–I.

511

512 **Figure 4—figure supplement 1.** Measuring lines on lichen-mimicking *L. ramimaculatus* and lichen *D.*
513 *ciliiferus*. (A) Measuring lines on the forewing of lichen-mimicking *L. ramimaculatus*,
514 CNU-NEU-NN2019004P. (B) Measuring lines on lichen specimen PB23120. (C) Measuring lines on
515 lichen specimen B0474. Measuring lines are indicated by their red color. Scale bars: 5 mm in A–C.

516

517 **Figure 5.** Habitus reconstruction of the lichen mimicking lacewing *Lichenipolystoechotes*
518 *ramimaculatus* gen. et sp. nov. on the lichen *Daohugouthallus ciliiferus* Wang, Krings et Taylor, 2010.

519 The colors used in the drawing of *D. ciliiferus* is Taupe, referring to the color of extant lichen
520 *Everniastrum cirrhatum*. The body of the *L. ramimaculatus* is reconstructed based on living ithonid
521 species, and the wing is based on the fossil of holotype CNU-NEU-NN2019006P/C. The color of insect
522 is yellowish-brown based on the general coloration of extant polystoechotids. Xiaoran Zuo did the
523 reconstruction drawing.

524

525 **Figure 6.** Lichen mimicry and camouflage by insects across major insect lineages. Time-dated
526 chronogram based on *Misof et al. (2014)*. Specific examples of fossil and modern lichen mimesis by
527 various insect taxa are provided at right. Black dots represent modern insect–lichen-mimetic
528 associations; the star represents the fossil *Lichenipolystoechotes*–lichen mimicry of this study.

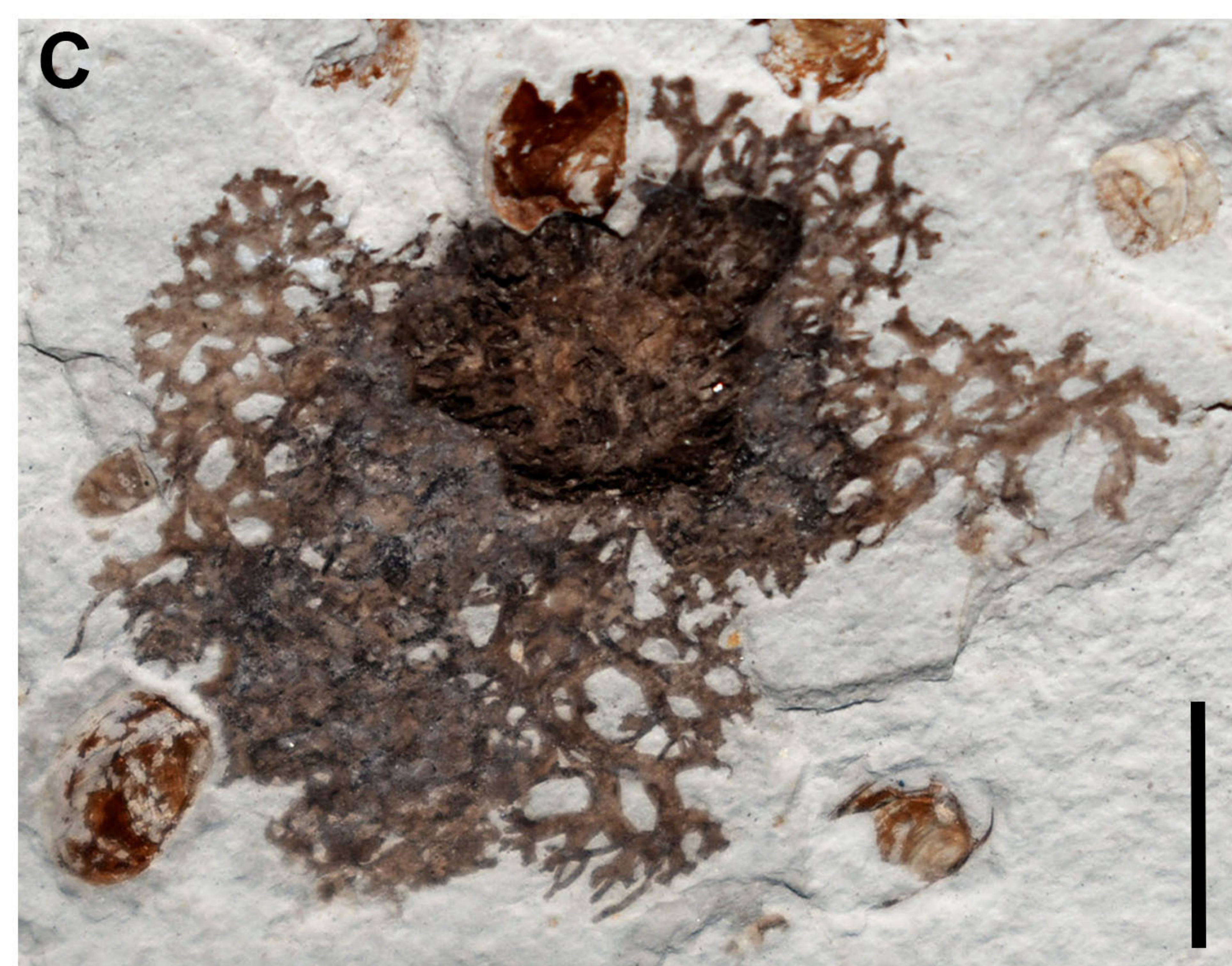
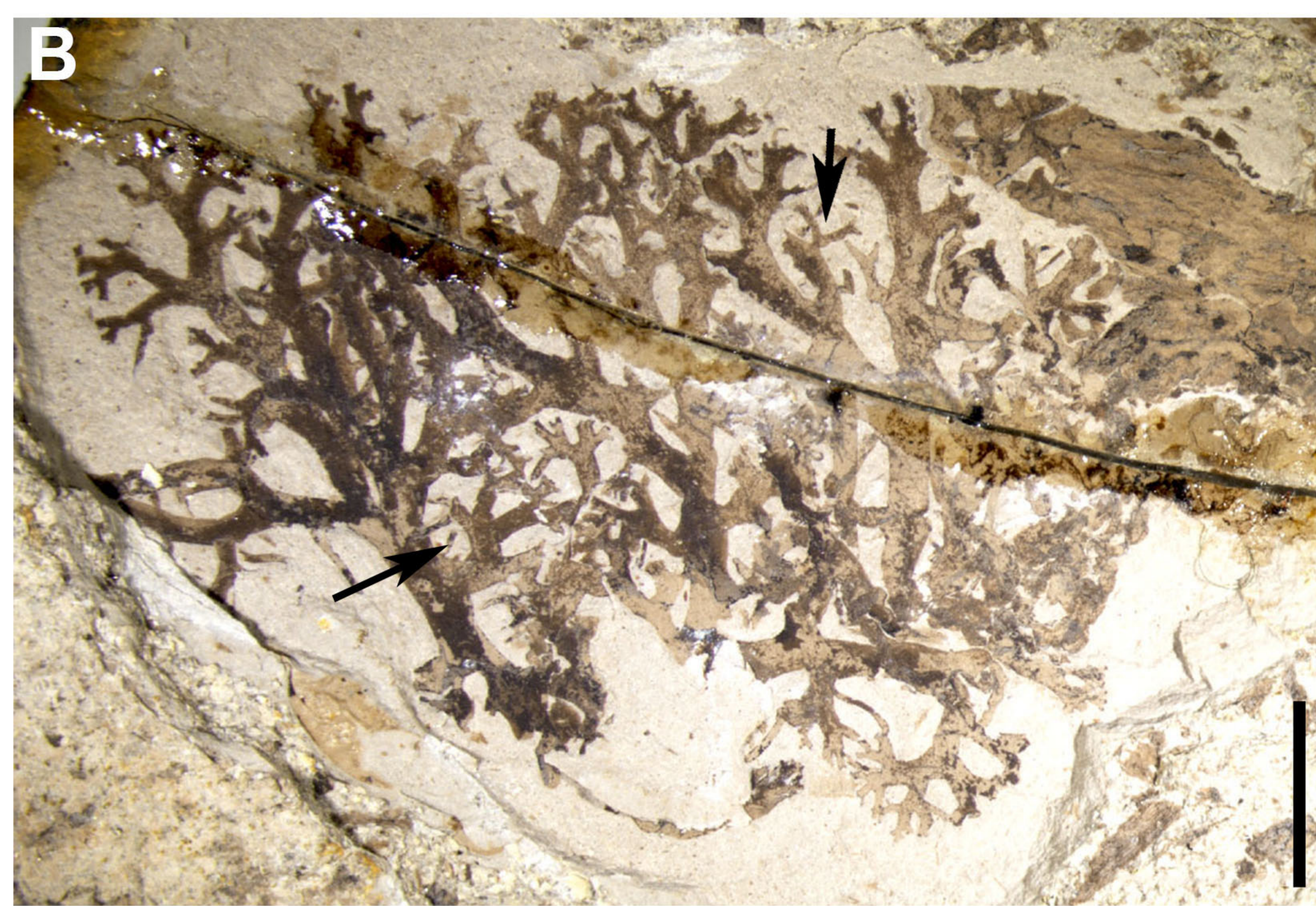
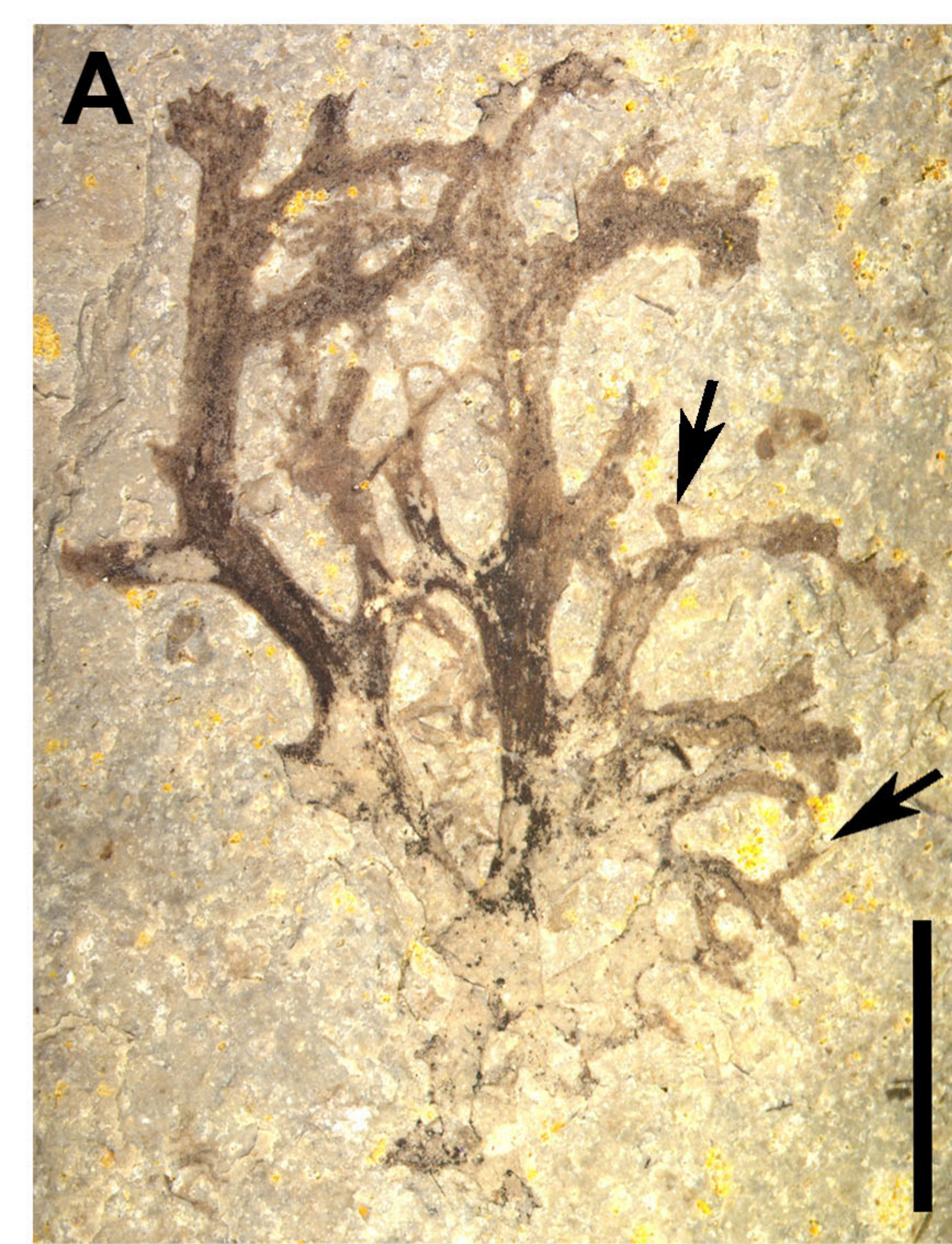
529

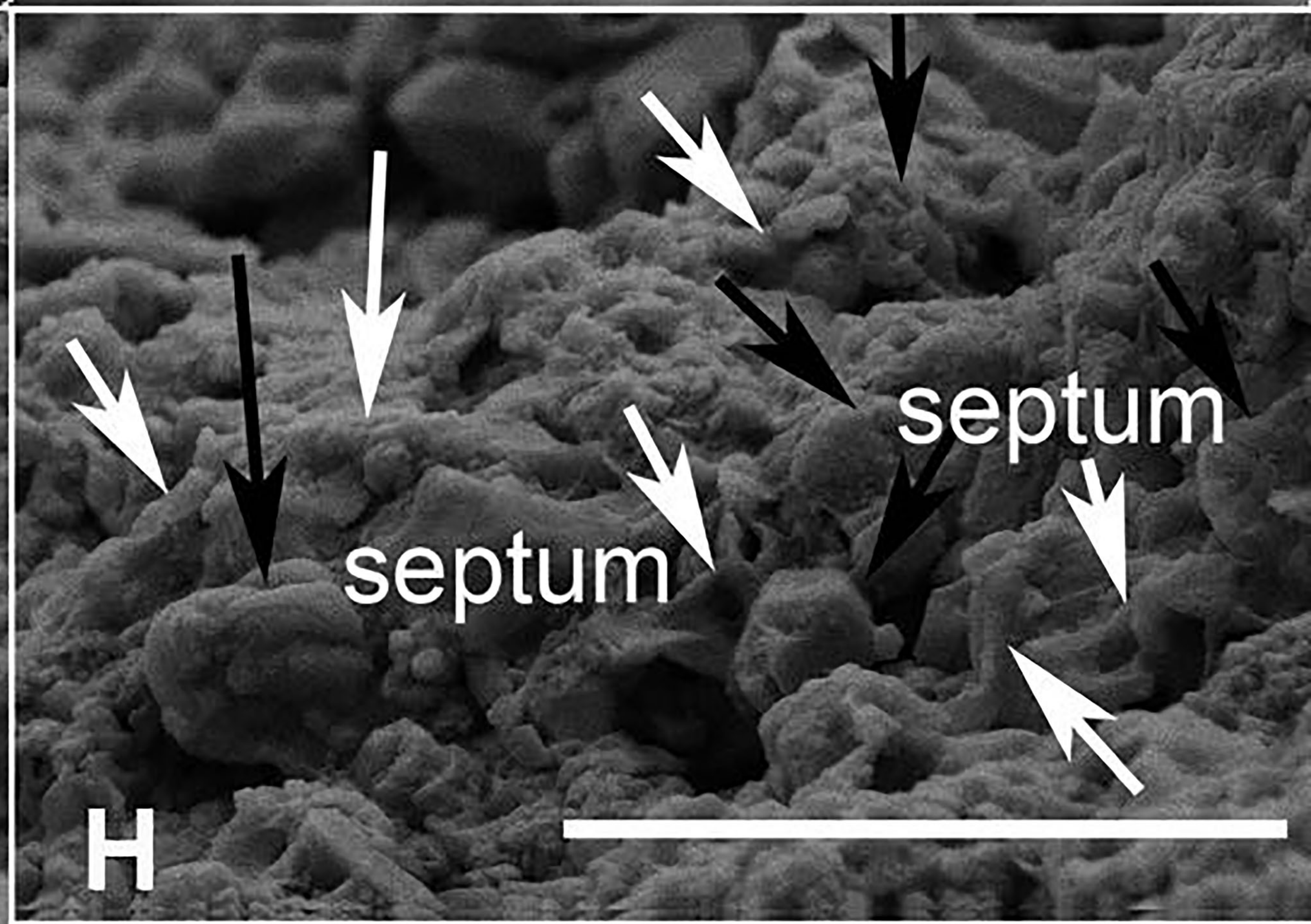
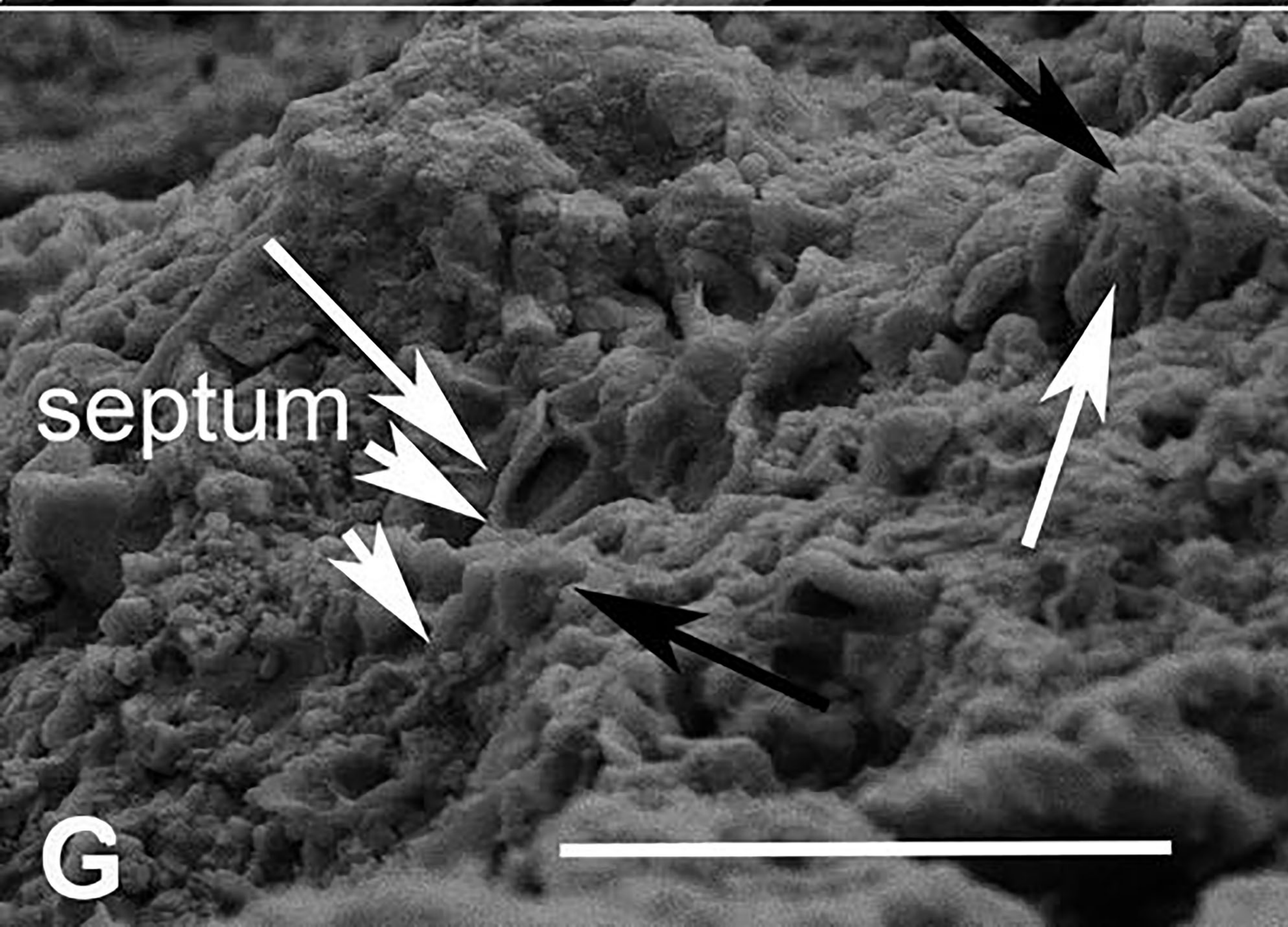
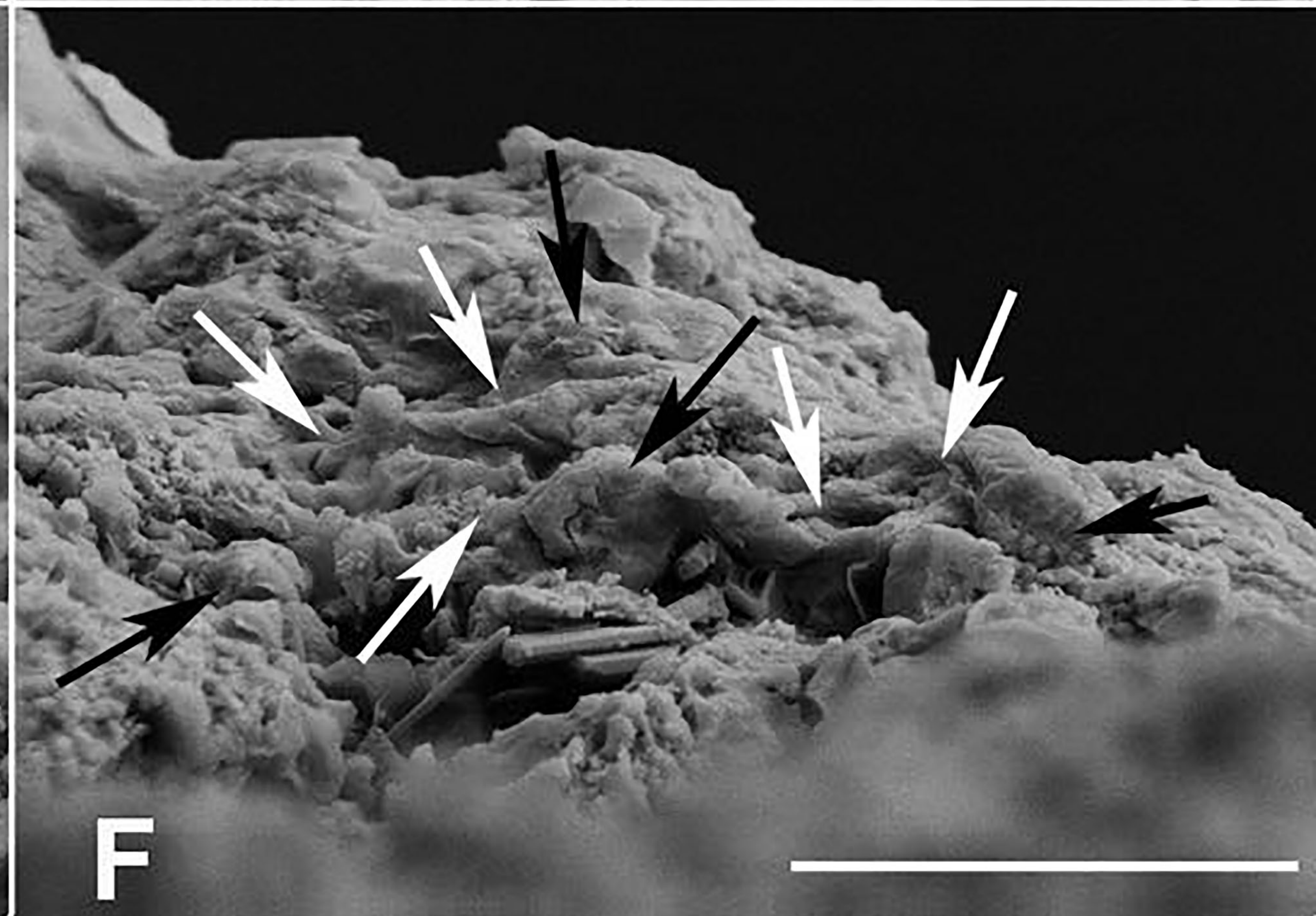
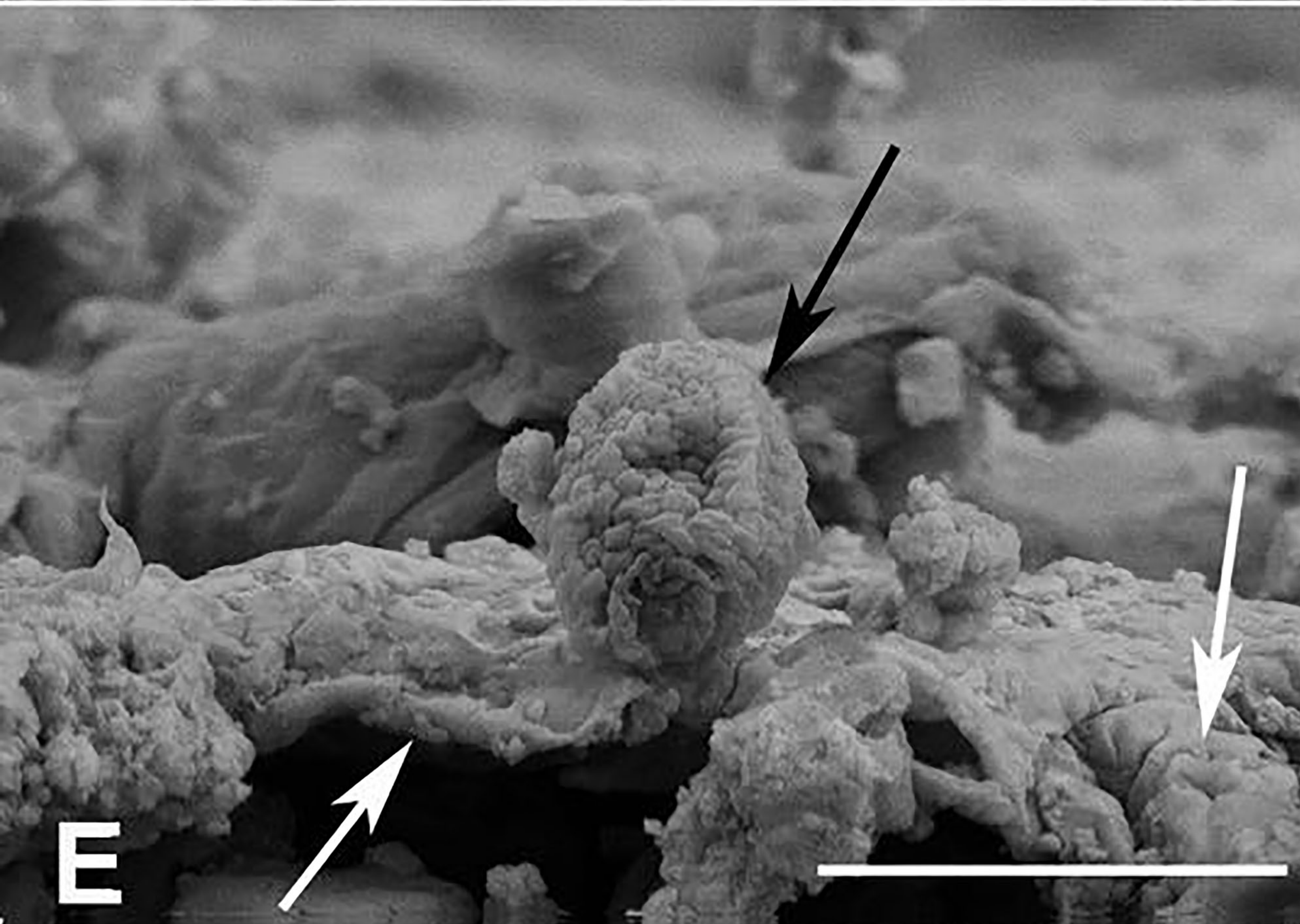
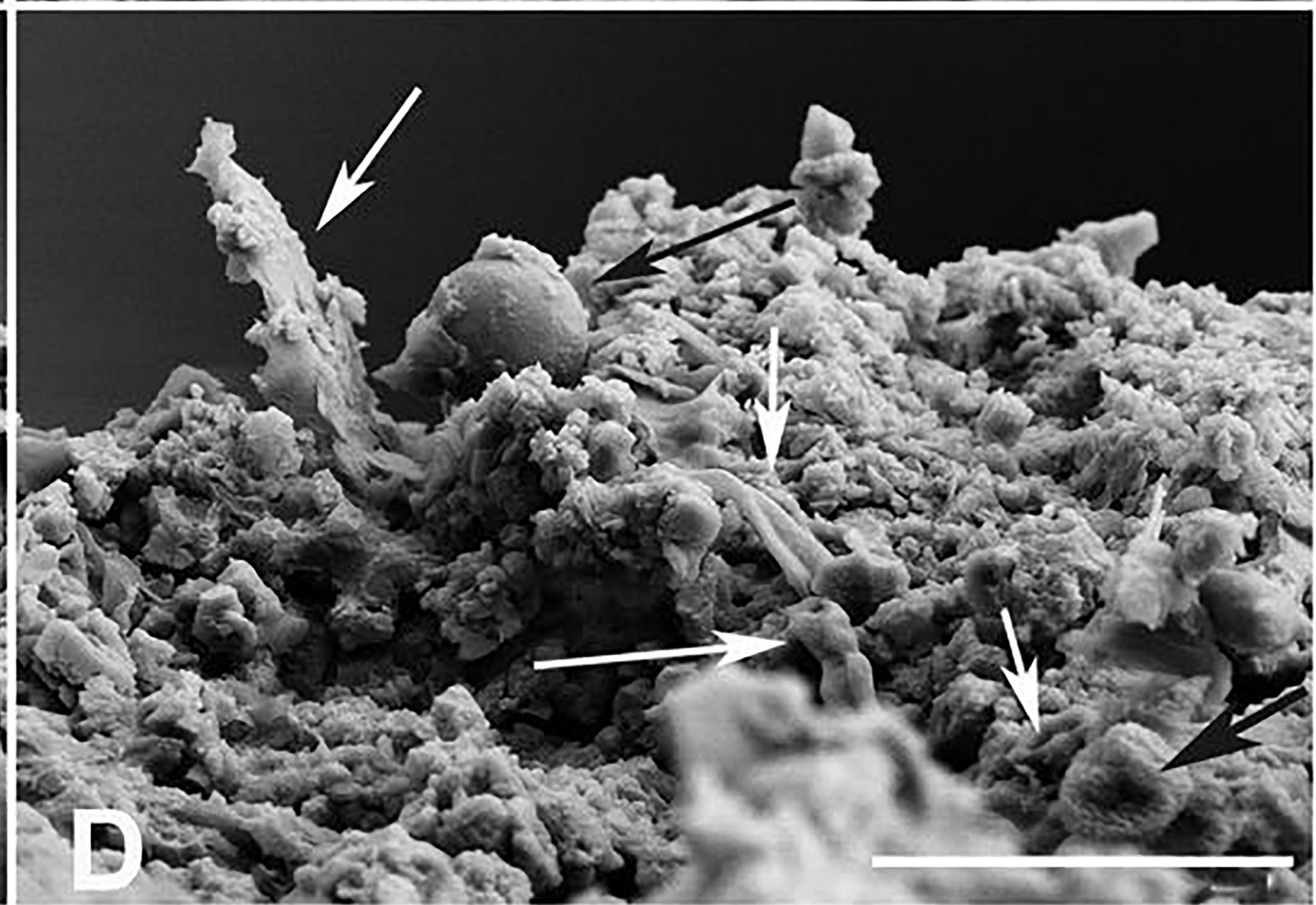
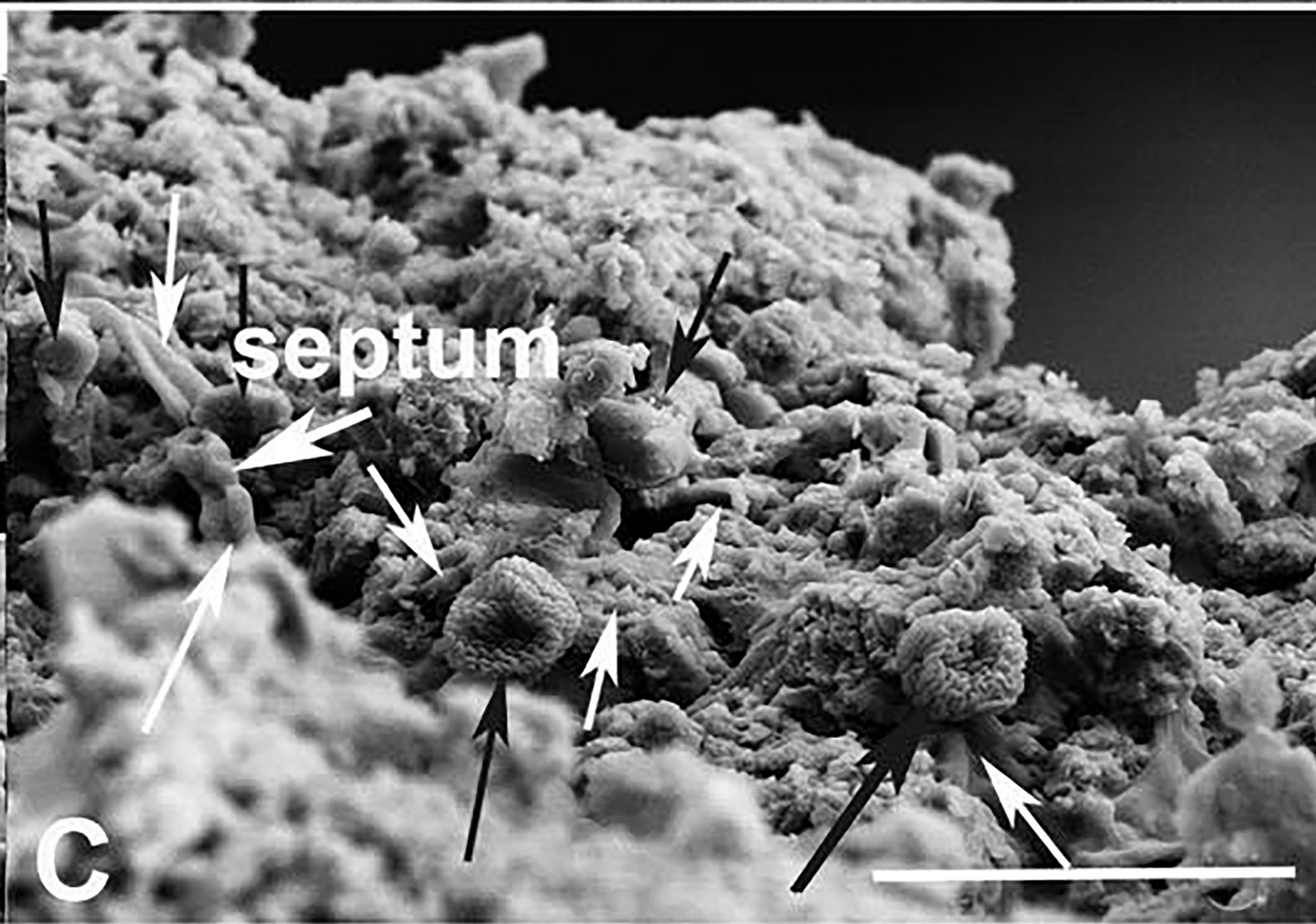
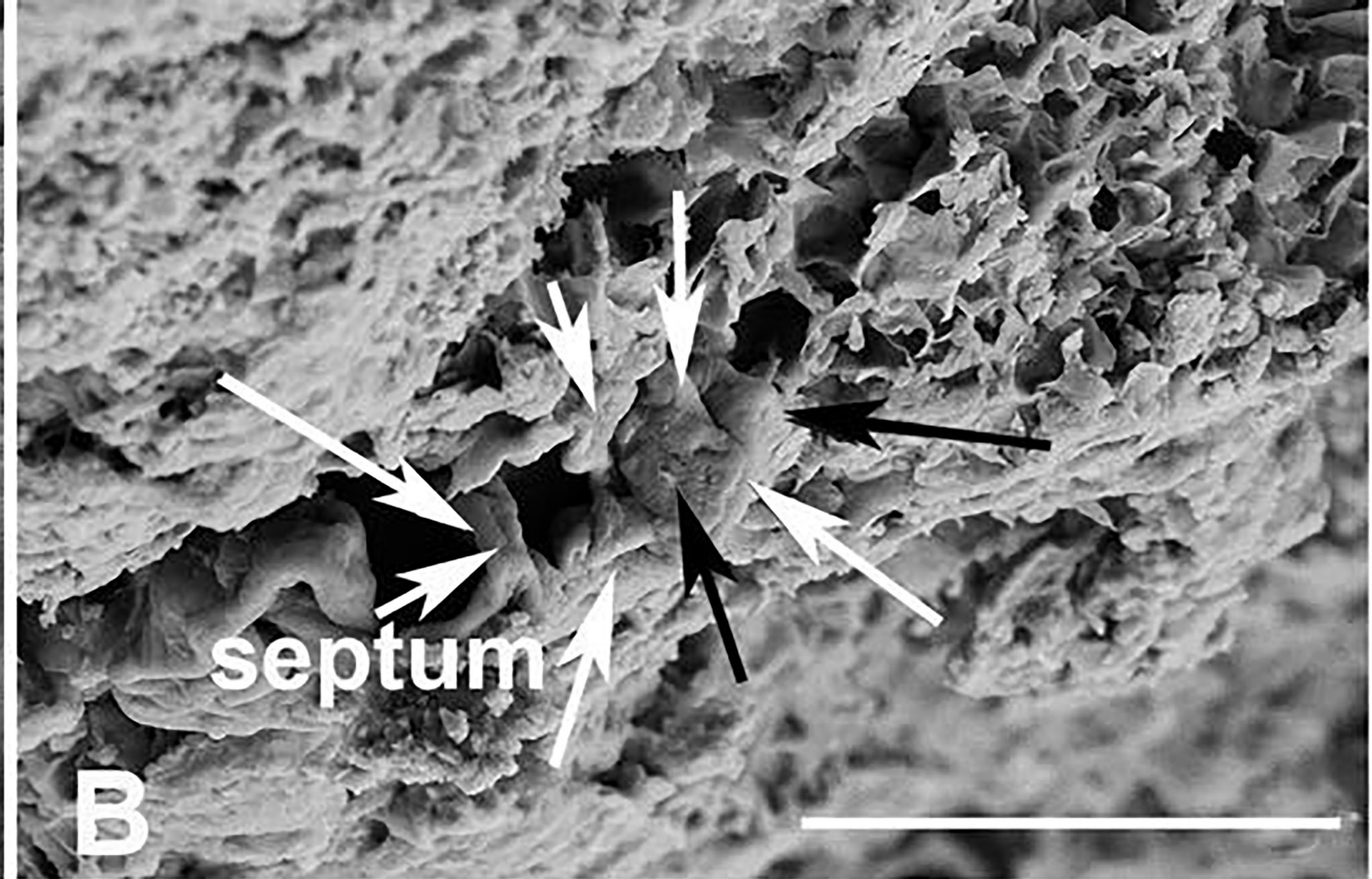
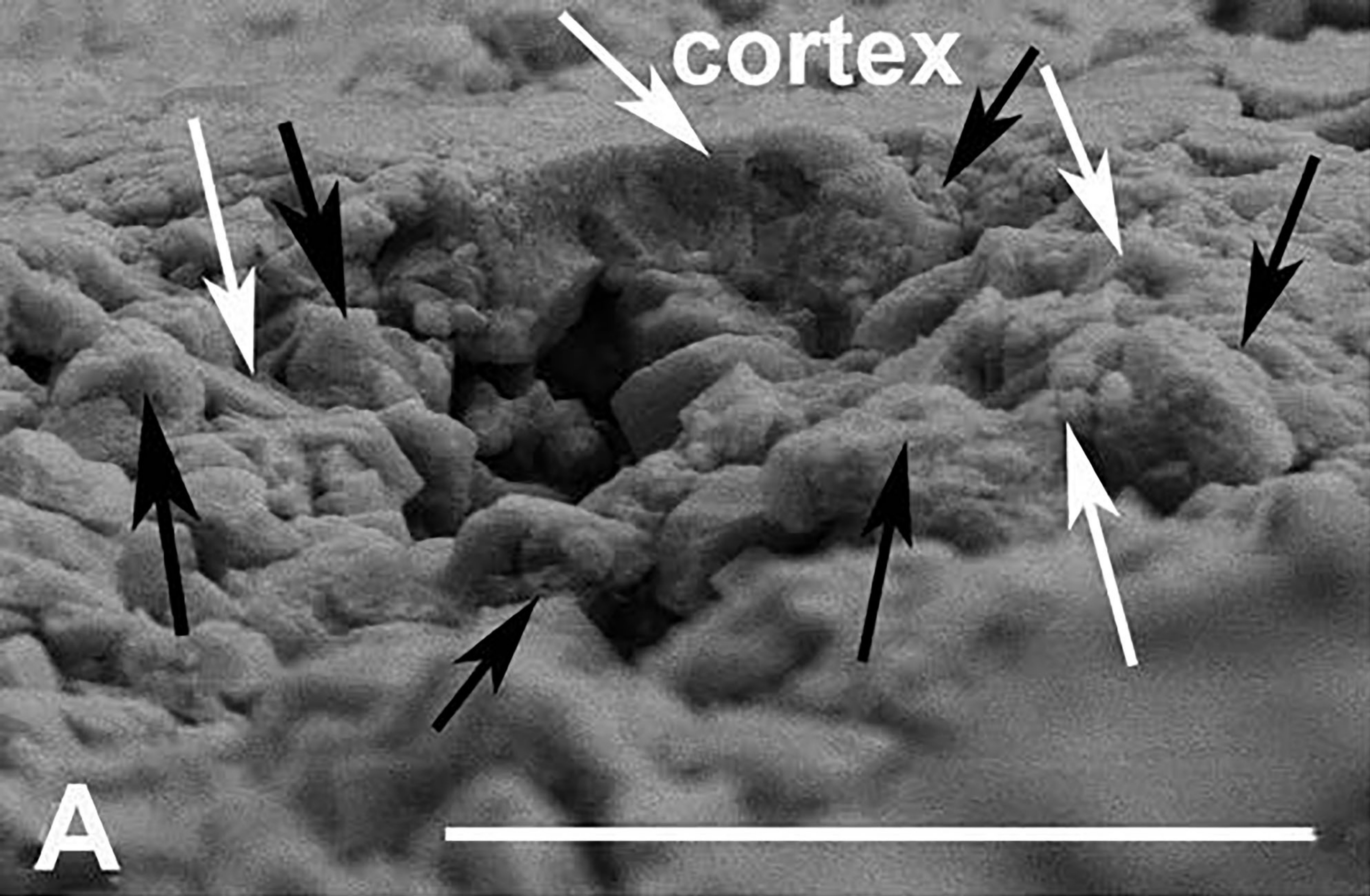
530 **Additional files**

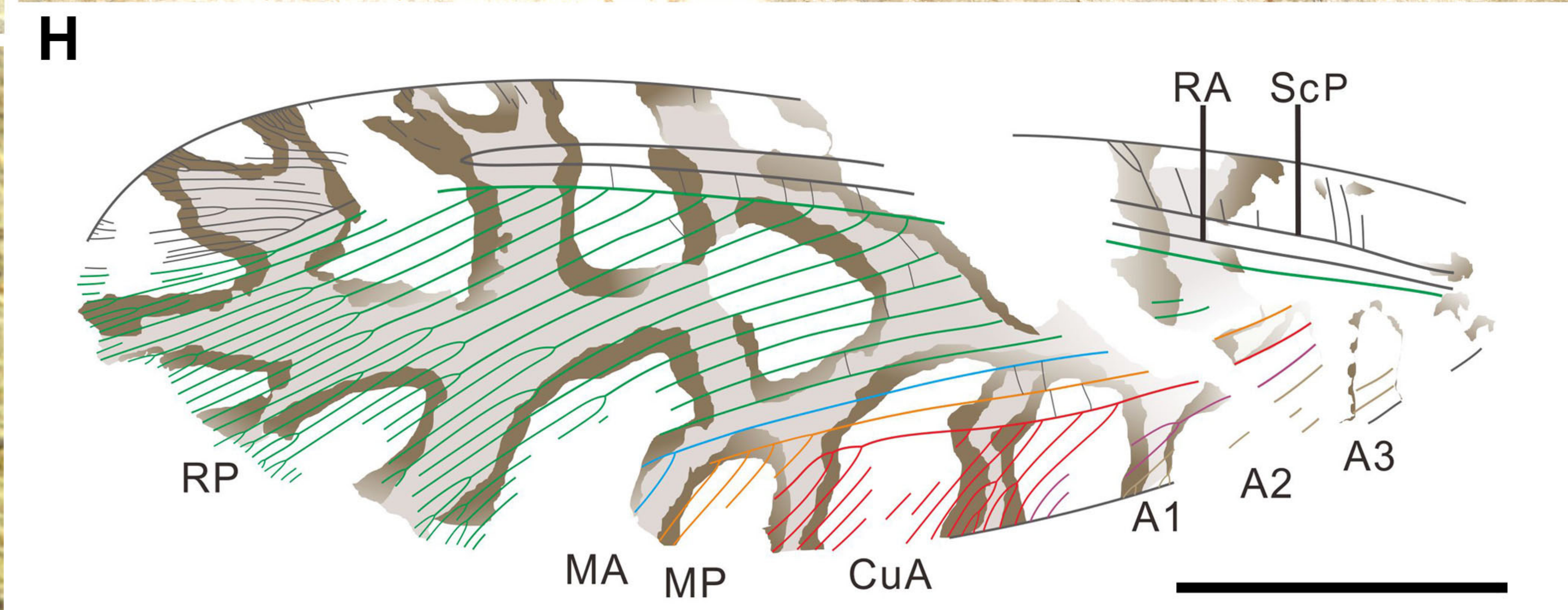
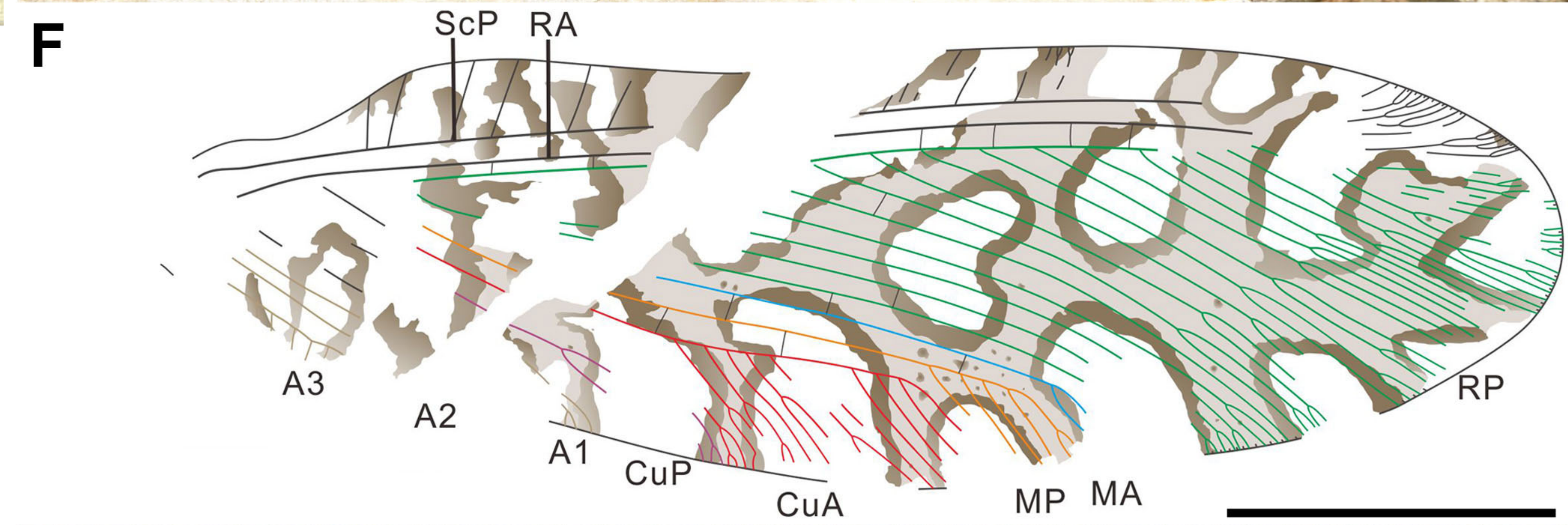
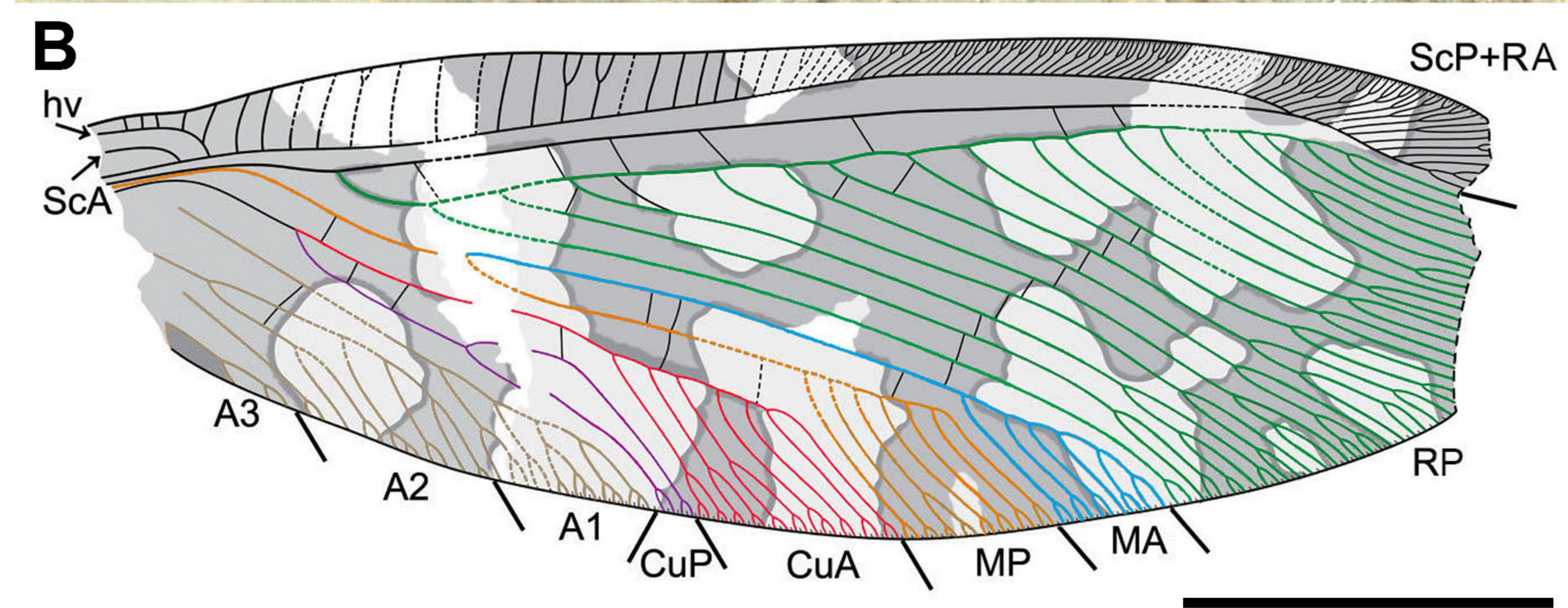
531 Supplementary files

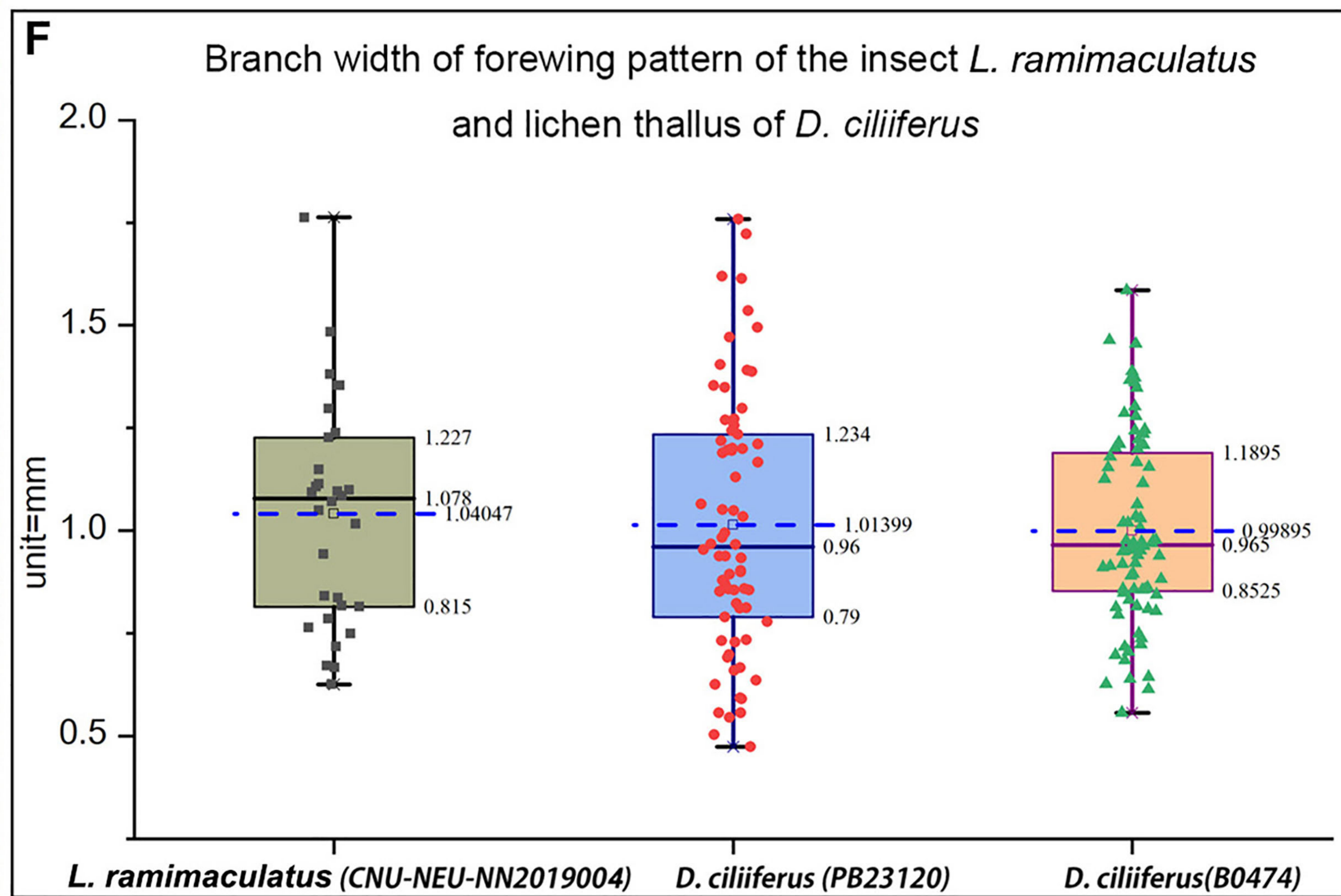
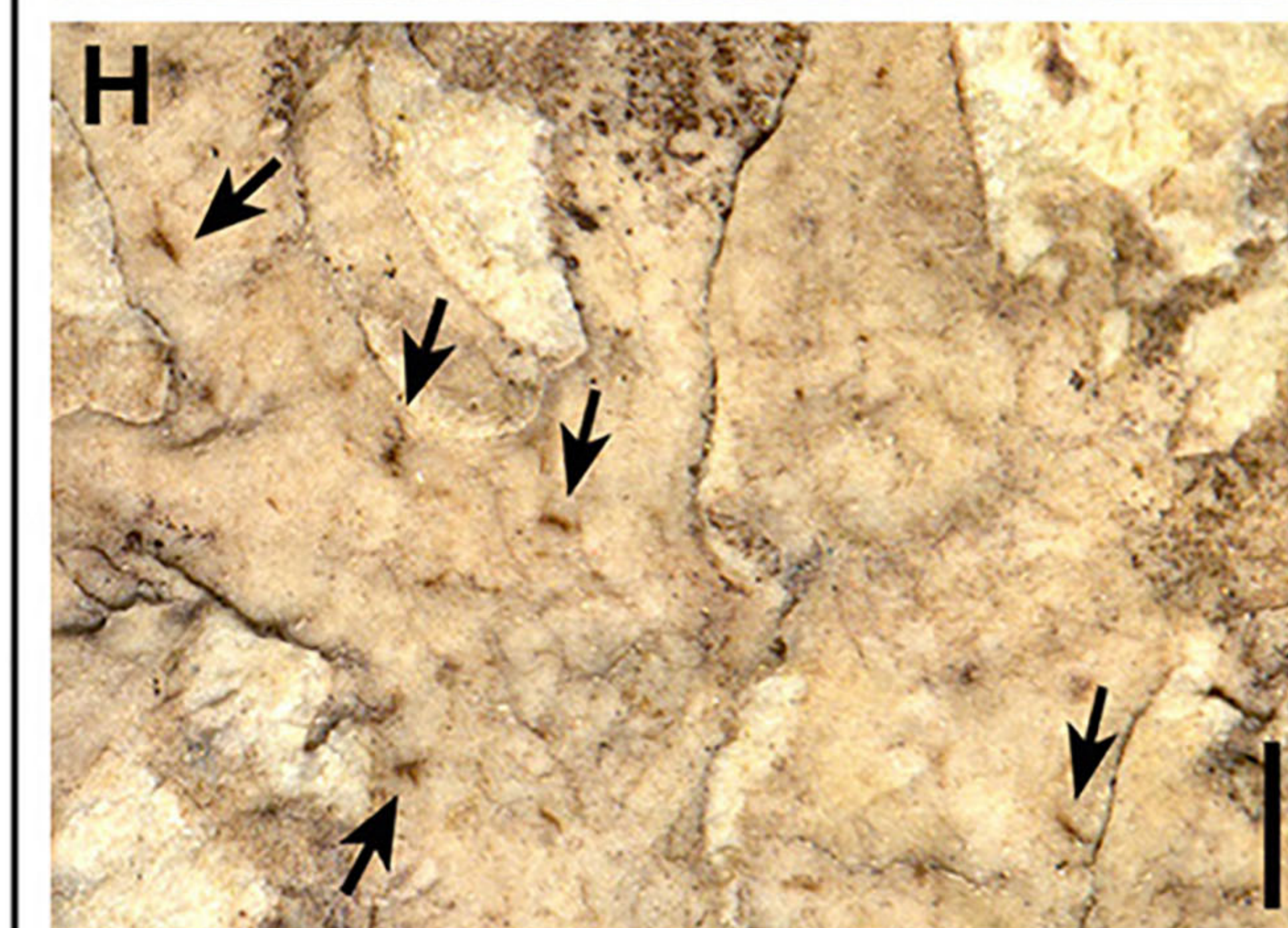
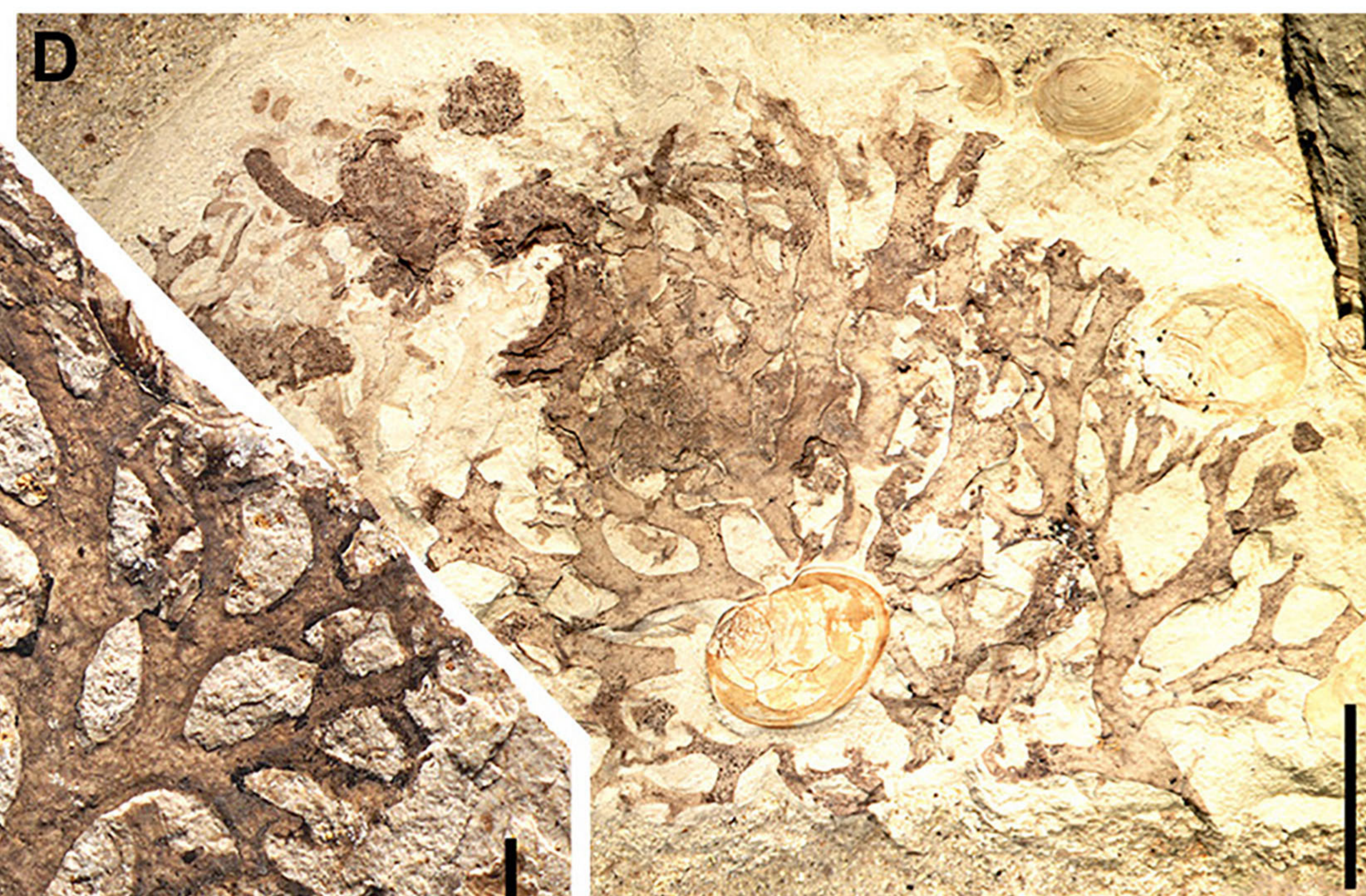
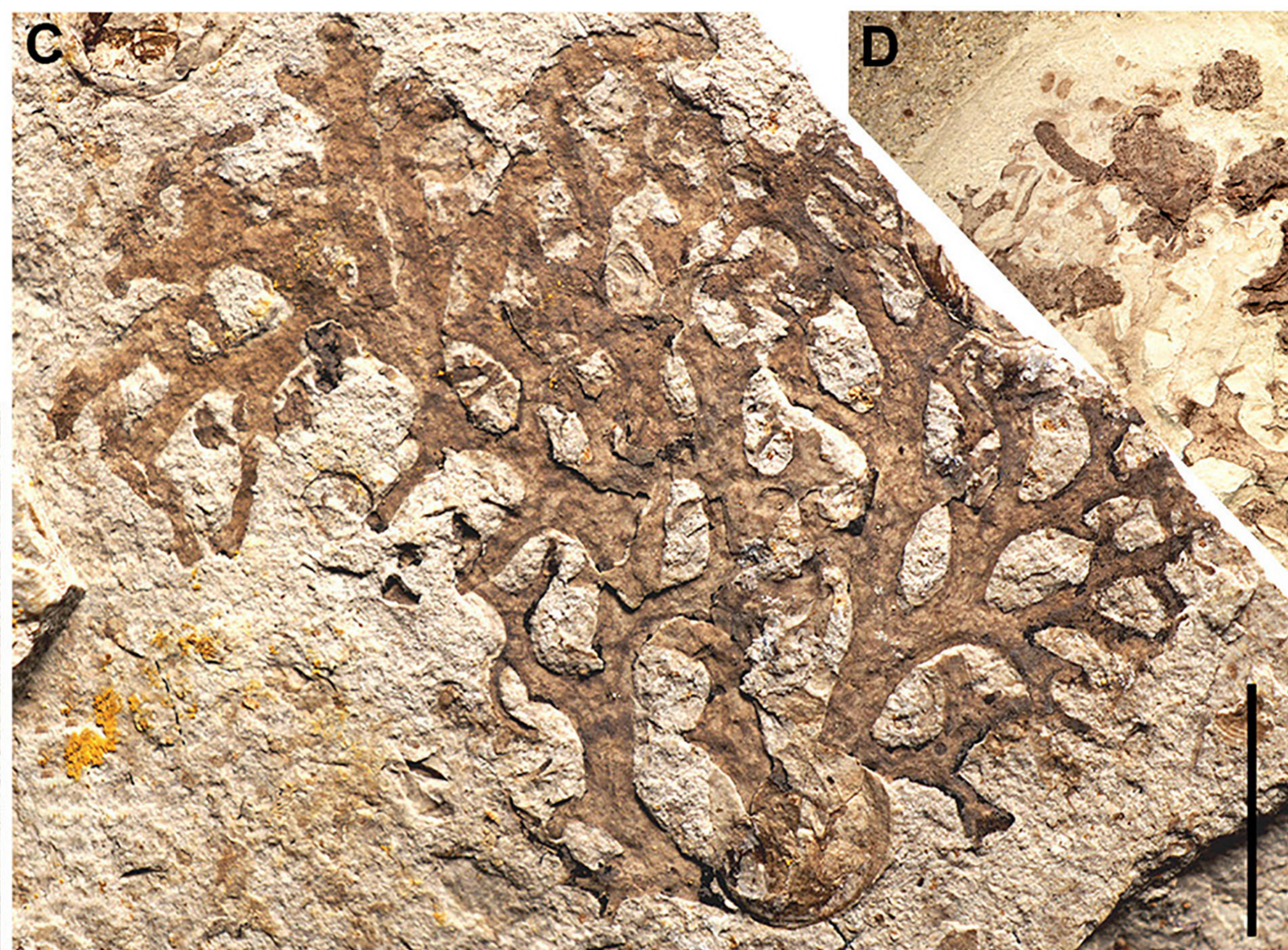
532 · Supplementary file 1. Table S1 Branch width of forewing pattern of

533 *Lichenipolystoechotes ramimaculatus* and lichen thallus of *Daohugouthallus ciliiferus*



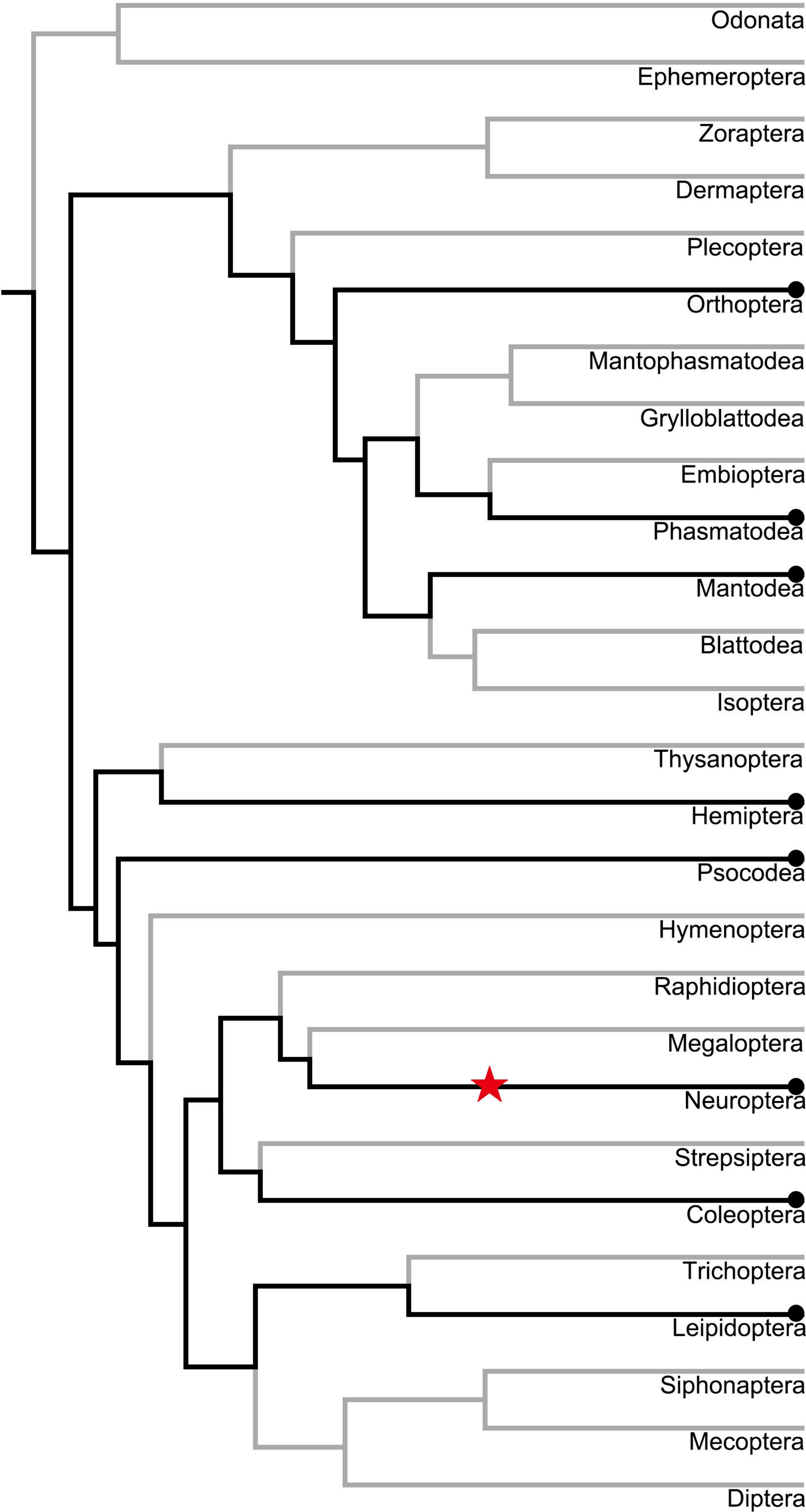
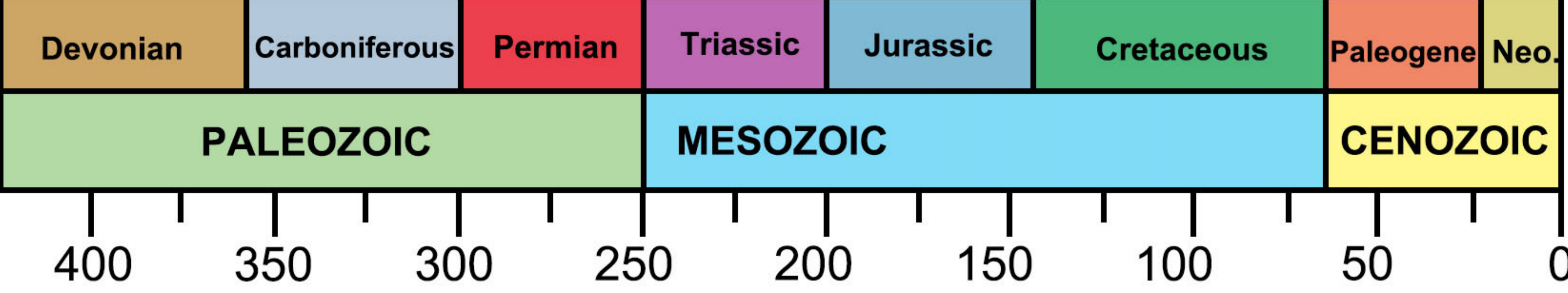












Grasshoppers and katydids:
Leuronotina, Lichenodraculus, Lichenagraecia etc.



Stick insects:
Extatosoma, Pseudodiacantha, Onchestus etc.



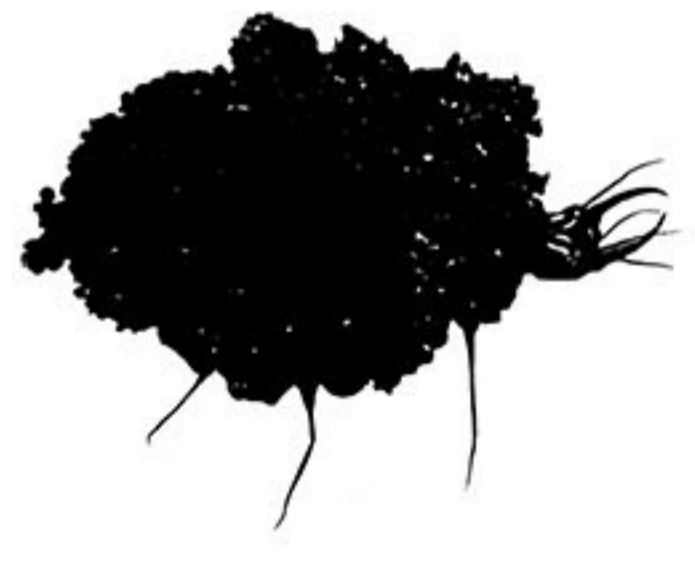
Mantids:
Gonatista



Bugs:
Phytocoris



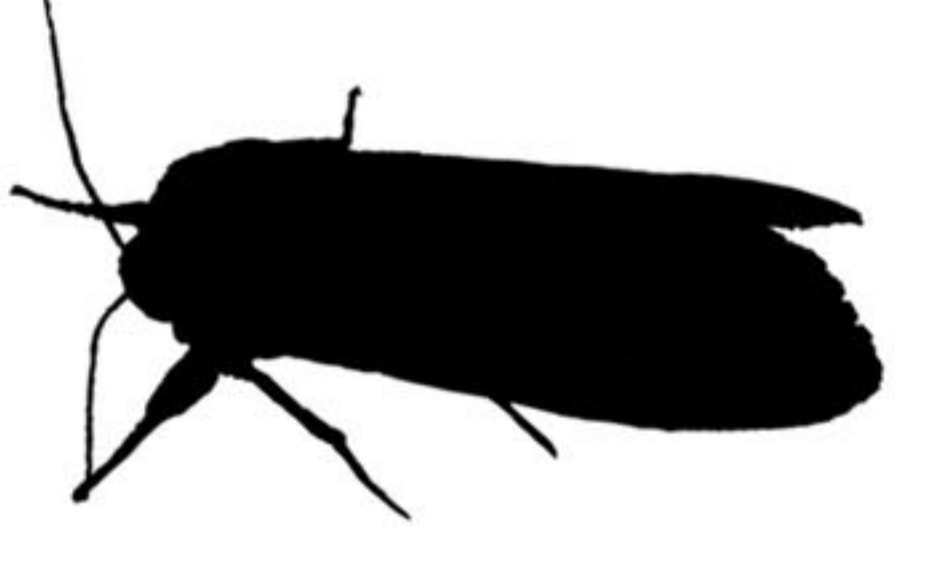
Psocids:
Trichadenotecnum



Lacewing larvae and adults:
debris-carrying *Leucochrysa* and *Ceraeochrysa*,
fossil *Lichenpolystoechotes*



Beetles and weevils:
Pristoderus, Synaphaeta, Pissodes



Moth larvae and adults:
Catocala, Macrurocampa, Leuconycta, Griposia etc.